RESEARCH ARTICLE

European Journal of
Lipid Science and Technology
www.ejlst.com

Spatial Recruitment of Cardiolipins in Inguinal White Adipose Tissue after Cold Stimulation is Independent of UCP1

Sebastian Dieckmann, Stefanie Maurer, Karin Kleigrewe, and Martin Klingenspor**

Brown and brite adipocytes are unique for uncoupling protein 1 (UCP1) dependent non-shivering thermogenesis (NST) induced by cold exposure. Several lipid species are associated with NST in brown and white adipose tissues (WAT). Studies investigating this association rely on the analysis of whole organ homogenates, or pre-adipocytes differentiated in vitro. These approaches do not account for the regional heterogeneity of WAT. The authors aimed to characterize the spatial lipid composition of WAT in an in vivo context to identify and validate lipids colocalized with UCP1. Therefore, matrix-assisted laser desorption ionization mass spectrometry imaging (MALDI-MSI), high-resolution mass spectrometry, and immunohistochemistry are applied on sections of inguinal WAT from UCP1 knockout and wildtype mice acclimatized to cold. The authors identified spatial overlap of cardiolipins and diacylglycerols in UCP1 positive regions, and triacylglycerols as the main lipid class characteristic for UCP1 negative regions within inguinal WAT. Investigation of UCP1 knockout and wildtype mice housed at room temperature or acclimatized to cold demonstrated that cardiolipins content in WAT is increased upon cold stimulation, independent of UCP1. In summary, a MALDI-MSI-based approach is introduced to identify lipids associated with thermogenic adipocytes in adipose tissues and demonstrate a regional cold-dependent upregulation of cardiolipins independent of UCP1. ***Practical application*****: It is demonstrated that MALDI-MSI is a valuable tool to investigate the spatial distribution of lipids in WAT. Consequently, it is an important complement to LC-MS/MS analysis of whole tissue homogenates. In combination with immunohistochemistry, it allows the straightforward examination of potential interactions between structural and metabolic traits, as demonstrated by spatial colocalization of UCP1 expression with specific lipid species in the current study. As a major advantage, this enables analyses on subsets of the same sample combining different analytic approaches, thereby potentially reducing the number of experimental animals.**

1. Introduction

Brownadipose tissue (BAT) is the main organ responsible for non-shivering thermogenesis (NST).[1,2] The distinctive cell type of BAT are brown adipocytes that are characterized by high expression levels of uncoupling protein 1 (UCP1), the key mediator of heat production.[1,2] NST capacity and UCP1 expression, however, are not restricted to BAT but are also recruited in brite adipocytes that emerge within inguinal white adipose tissue (iWAT) upon prolonged β_3-adrenergic signaling in a process termed "browning".[3] The thermogenic function of brown and brite adipocytes is not only linked to UCP1 expression, but also to the cellular morphology and ultrastructure of these adipocytes.[4] Both cell types contain multilocular lipid droplets in contrast to the mostly unilocular appearance of lipid droplets in white adipocytes,[4] the main cell type for storing excessive energy in form of triglycerides. Brown and brite adipocytes are packed with mitochondria that are required to enable high rates of ATP-independent uncoupled respiration but also ATP-dependent futile cycles.[5] In contrast to white adipocytes, brown and brite adipocytes exhibit high capacities for de novo lipogenesis, beta-oxidation, lipolysis, and re-esterification of fatty acids.[2] Consequently, quantitative lipidomics revealed substantial differences of brown and brite adipocytes as compared to white adipocytes, with higher levels of

S. Dieckmann, S. Maurer, M. Klingenspor
Chair for Molecular Nutritional Medicine
TUM School of Life Sciences
Technical University of Munich
Freising 85354, Germany
E-mail: mk@tum.de

DOI: 10.1002/ejlt.202100090

S. Dieckmann, S. Maurer, M. Klingenspor
EKFZ – Else Kröner-Fresenius Center for Nutritional Medicine
Technical University of Munich
Freising 85354, Germany

S. Dieckmann, S. Maurer, M. Klingenspor
ZIEL – Institute for Food & Health
Technical University of Munich
Freising 85354, Germany

K. Kleigrewe
Bavarian Center for Biomolecular Mass Spectrometry (BayBioMS)
Technical University of Munich
Freising 85354, Germany
E-mail: karin.kleigrewe@tum.de

distinct phospholipid classes, diacylglycerols, and cardiolipins (CL) in these thermogenic adipocytes.[6–9] CL is an essential component of the inner mitochondrial membrane. They are composed of two phosphatidylglycerols linked by glycerol, forming a dimeric phospholipid with four acyl chains. Bound to several mitochondrial membrane proteins, CL is a signature lipid class of mitochondria and plays a pivotal role in mitochondrial functionality.[10] Pathological alterations in CL metabolism are linked to several diseases such as Barth syndrome, myocardial ischemia, Parkinson's disease, or diabetes.[10] The importance of CL in mitochondrial bioenergetics results from the interaction with enzymes of the electron transport chain and the ATP synthase.[10] Further, CL is functionally relevant for NST,[7] induced in brown adipocytes upon ß3-adrenergic signaling and essential for small rodents to defend body core temperature.[2] Induction of brite adipogenesis of immortalized pre-adipocytes results in changes of CL composition.[11] Stimulation of brown and brite adipocytes by β_3-adrenergic receptor agonists increases the CL content in brite and brown adipocytes in vitro as well as in iWAT and BAT in vivo.[6–9] The association between CL and UCP1 is further demonstrated by the stabilizing effect of CL on UCP1,[12,13] facilitating its function. In line, adipose tissue specific knockout of cardiolipin synthase 1 impairs the ß3-adrenergic induced recruitment of UCP1.[7]

Although the significance of CL for UCP1 function is well established, the impact of UCP1 on CL abundance has not been studied, so far. Further, the studies investigating changes in lipid composition and the association between CL and BAT activity or UCP1 rely on the analysis of whole organ homogenates,[7–9] or on the differentiation of pre-adipocytes in vitro.[6,11] Considering the heterogeneity of white adipose tissue (WAT),[14] these approaches might neglect region-specific differences in lipid metabolism. Consequently, we asked whether changes in the lipid profile in respect to CL occur ubiquitously in WAT or in a spatial pattern coinciding with the presence of brite adipocytes and their expression of UCP1. Therefore, the aim of our study was to characterize the lipid composition of adipose tissue and to demonstrate the association between CL and UCP1 on a region-specific level in an in vivo context. We established MALDI mass spectrometry imaging (MALDI-MSI) in combination with immunohistochemistry (IHC) and high-resolution LC-MS/MS as a suitable approach to identify lipids associated with specific functions like the cold-induced recruitment of thermogenic adipocytes.

2. Experimental Section

2.1. Animals

All animals were bred and housed in a specific pathogen-free facility at 23 °C ambient temperature. The experiments were performed according to the German animal welfare law with permission from the district government of Upper Bavaria (Regierung von Oberbayern, reference number ROB-55.2-2532.Vet_02-16-166). At the age of 8-weeks, male mice were single caged, transferred to climate cabinets set to 23 °C and 55% relative humidity. Simultaneously, mice were switched to a control diet (Snifff Cat. No S5745-E702). Two independent experiments were performed with two different mouse strains (129S6/SvEvTac & C57BL/6N).

2.1.1. 129S6/SvEvTac

After 3 weeks at 23 °C, all mice were directly transferred into a second climate cabinet set to 5 °C ambient temperature and 55% relative humidity for 1 week.

2.1.2. C57BL/6N

UCP1-knockout (UCP1-KO) and wildtype (UCP1-WT) mice on a C57BL/6N background were generated in the EUCOMM program[15,16] as described previously.[17] All mice were derived from heterozygous (UCP1-HET) breeding pairs. At the start of the experiment, mice were divided into two groups matched by genotypes and body weights. One week after transfer to the climate chambers at 23 °C, one group (5 °C) was acclimatized stepwise to cold by decreasing the ambient temperature weekly to 20, 15, 10, and finally 5 °C, while the second group (23 °C) was maintained at 23 °C during this 4-week-period.

All mice were killed by asphyxiation in CO_2 anesthesia and severing of the diaphragm. iWAT was dissected, weighed, and immediately embedded in 1% carboxymethylcellulose on dry ice. Tissues were stored at −80 °C until further processing.

2.2. Cryosectioning

Cryosections of iWAT were generated with a Leica CM2505 Cryostat set to −35 °C chamber temperature and −30 °C specimen temperature. To obtain sections of similar regions within the tissue, approximately 20–25 16 µm thick sections were discarded until the lymph node was visible in the sections. Subsequently, 6 consecutive 16 µm sections were obtained. The first section was thaw mounted on a chilled conductive ITO-slide (Bruker Daltonik, Bremen). The second section was thaw mounted on a polysine-coated slide for IHC. The third and fourth sections were combined and transferred into a glass vial for LC-MS/MS analysis. A fifth and sixth section were discarded before sectioning of the next replicate. Samples on ITO-Slides and in glass vials were kept within the cryostat. Samples for IHC and H&E staining were kept at room temperature. After preparation of all samples, teaching points were drawn on the ITO-slide with a correction pen (Tipp-Ex, BIC, Cat. No. 8022921). An image of the dried ITO-slide was acquired with a digital single-lens reflex camera (Nikon D5600) for alignment with the MALDI instrument. Subsequently, all slides were placed in a vacuum desiccator, evacuated for 10 min, and closed and dried for additional 20 min at room temperature. The ITO-slide was immediately processed further for MALDI-MSI (matrix application), while all other slides were stored at −20 °C until staining. Samples in glass vials were stored at −80 °C until further processing.

2.3. Matrix Application

The HCCA matrix (7 g/l HCCA, 0.2% TFA in 60% ACN) was applied on ITO-slides by spraying (ImagePrep, Bruker Daltonik, Bremen) and the following program: 1) Initialization, 2) 0.07 V, 1 cycle, 0.05 V, 3) 0.07 V, 2 cycle, 0.1 V, 4) 0.2 V, 3 cycle, 0.2 V, 5) 0.6/−0.5 V, 4 cycle, 0.3 V.

2.4. MALDI-MSI

MALDI-MSI was performed on the MALDI ultrafleXtreme (Bruker Daltonik, Bremen, Germany) with a Smartbeam2-Laser set to "4 large" and a raster size of 100 µm in positive ionization mode.

2.5. Immunohistochemistry (IHC)

Samples on polysine-coated slides were washed 5 min in tris-buffered saline (TBS) and fixed for 10 min in ice-cold methanol/acetone (1:1). Fixed samples were washed twice in TBS for 5 min. Blocking was performed for 2 h at room temperature (RT) (TBS, 0.1% Tween-20 (TBST) with 10% donkey serum, 1% bovine serum albumin) before application of the primary antibody against UCP1 (1:800, Abcam, Cat. No. ab23841) for 2 h at RT or overnight at 4 °C. After primary antibody incubation, samples were washed three times in TBST for 5 min before applying the secondary antibody (1:500, Thermo Fisher, Cat. No. A10040) overnight at 4 °C or 2 h at RT. Secondary antibody solution was removed and samples stained with Hoechst33342 (1:500, Sigma, Cat. No. 14 533) for 10 min at RT. Finally, samples were washed three times in TBST for 5 min, supplied with mounting medium (Biozol, Cat. No. VEC-H-1000-10), covered by a cover slide, and sealed with nail polish. Whole slide scans were performed immediately after staining with a fluorescence microscope (Leica AF000 LX, Filters: Y3 ET, Cat. No. 11504169 and DAPI ET, Cat. No. 11504203). Merged slide scans were exported from the LAS X software and subsequently opened and edited identically in ImageJ (Version 1.53c).

2.6. LC-MS/MS Analysis

The tissue section was extracted with 0.5 mL chloroform/methanol (1:1, v:v) in an analytical glass vial. First, each tissue section was vortexed for 30 s with a centrifugation step for 1 min at 1200 rpm. Afterward, the samples were sonicated for 15 min and shaken for 30 min. After centrifugation for 5 min at 3000 rpm, 200 µL of the supernatant was dried in a Concentrator plus (Eppendorf) and dissolved in 20 µL chloroform/methanol (1:1, v:v) which was used for analysis.

The lipid analysis was performed using a Nexera UHPLC system (Shimadzu) coupled to a Q-TOF mass spectrometer (TripleTOF 6600, AB Sciex) according to a published analytical method:[18] Separation of the lipid extract was performed using a UPLC BEH C18 2.1 × 100, 1.7 µm analytical column (Waters Corp.) with 300 µL min^{-1} flow rate. The mobile phase was water/acetonitrile (40:60, v:v) with 10 mM ammonium formiate and 0.1% formic acid (eluent A) and isopropanol/acetonitrile (90:10, v:v) with 10 mM ammonium formiate and 0.1% formic acid (eluent B). The gradient profile was 32% B from 0 to 1.5 min raising to 97% B at 21 min which was held for 4 min. Afterward, the column was equilibrated at starting conditions. A volume of 5µL per sample was injected. The autosampler was cooled to 10 °C and the column oven heated to 40 °C. The samples were measured in the Information Dependent Acquisition (IDA) mode. MS settings in the positive mode were as follows: Gas 1 55, Gas 2 65, Curtain gas 35, Temperature 500 °C, Ion Spray Voltage 5500, declustering potential 80. The mass range of the TOF MS and MS/MS scans were 100–2000 m/z and the collision energy set to 35 V with a 15 V spread. MS settings in the negative mode were as follows: Gas 1 55, Gas 2 65, Cur 35, Temperature 500 °C, Ion Spray Voltage −4500, declustering potential −80. The mass range of the TOF MS and MS/MS scans were 100–2000 m/z and the collision energy set to −35 V with a 15 V spread. Mass to charge ratios identified by MALDI were added to the inclusion list to obtain a respective MS/MS-spectra for lipid annotation by MS-DIAL.[19]

2.7. Data Analysis

Analysis of data acquired by MALDI-MSI was performed with the SCiLS software (Bruker Daltonik, Bremen, Germany, Version 2016b) and the tools provided with the software. Sections of one measurement were loaded as individual regions in a combined dataset, applying convolution baseline correction. Data were normalized to the total ion count for data analysis and image representation. Labels of intensity plots (Figure 3D,F) have been modified for graphical representation using inkscape (https://inkscape.org). Segmentation was performed on medium denoised data by top-down clustering using bisecting k-means similar to the method described by Alexandrov and coworkers.[20] Discriminative m/z intervals were identified by receiver operating characteristic (ROC) analysis with the built-in tool of the SCiLS software—"Find discriminative m/z values (ROC)". This tool calculates the area under the ROC curve (AUC_{ROC}) to assess the discrimination quality of all m/z values for two defined groups, where AUC_{ROC} values close to 0.0 and 1.0 indicate good discrimination, while values close to 0.5 suggest no discrimination between the groups.

Initial annotation of m/z intervals was based on the bulk search option of the LIPID MAPS Structure Database (LMSD) considering only $[M+H]^+$ ions with a mass tolerance of ±0.5 Da (https://www.lipidmaps.org/resources/tools/bulk_structure_searches.php?database = LMSD). LC-MS Data was analyzed with the MS-Dial software (Version 4.48[19]).

3. Results

3.1. MALDI-MSI Yields Reproducible Results within Different Sections of iWAT

The iWAT is a heterogeneous tissue, showing region-specific degrees of browning.[14] Due to this heterogeneity studies on whole tissue homogenates cannot resolve regional changes in the lipidomic profile induced by various treatment conditions. The aim of our study was to address this issue by applying MALDI-MSI on sections of iWAT. The heterogeneity within the tissue potentially sets limitations to the interpretation of results. Reproducibility may be hampered by the comparison of sections taken in different depths in the tissue. We established the reproducibility and comparability on iWAT of 129S6/SvEvTac mice acclimatized to 5 °C for 1 week. Mice of the 129S6/SvEvTac strain were used due to their high browning propensity. As a first step to reduce the variability between measurements, we restricted the

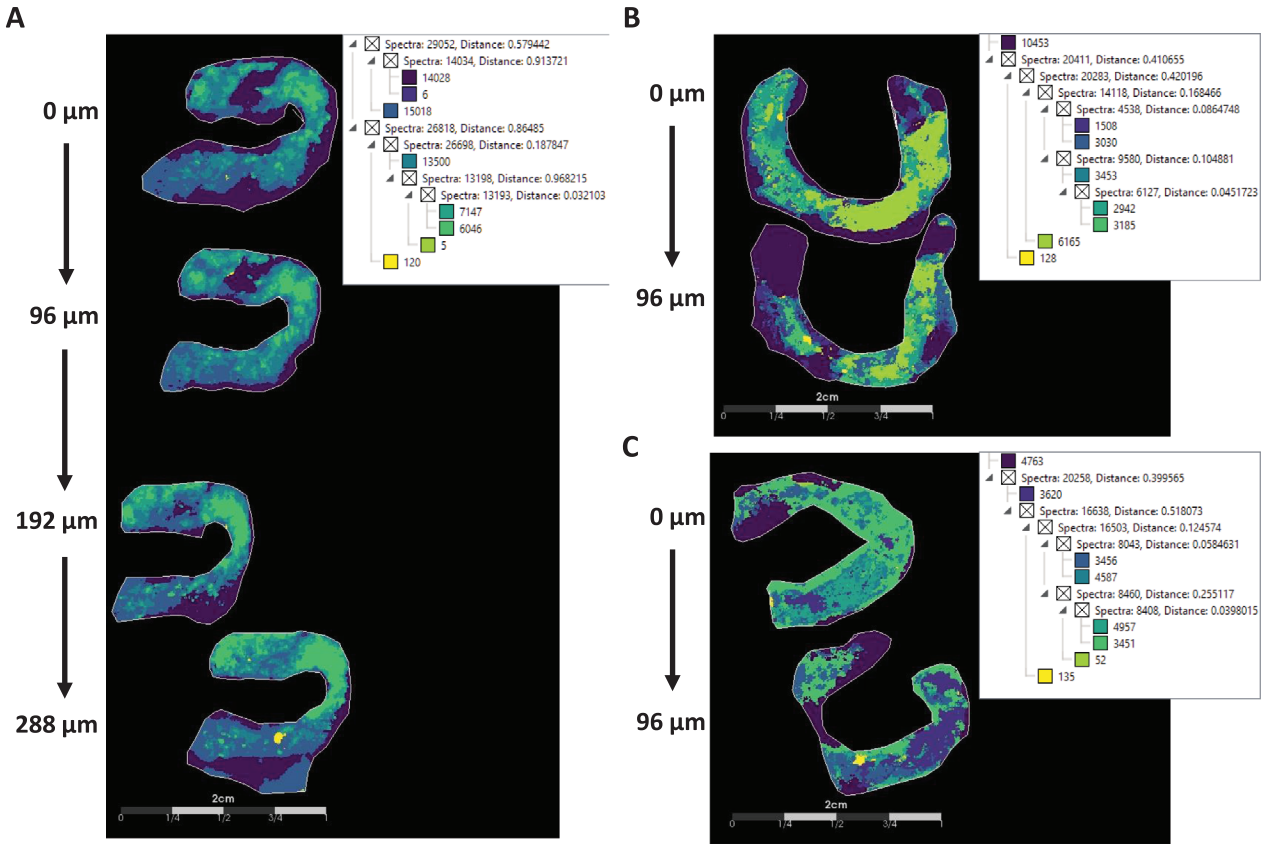

Figure 1. High similarity between different sections. Segmentation results of iWAT of three (A–C) 129S6/SvEvTac mice acclimatized to 5 °C for 1 week. Sections spanning a range of B,C) ≈100 µm up to A) ≈280 µm subjected to MALDI-MSI with subsequent spatial segmentation based on bisecting k-means in combination with correlation distance. Identical colors indicate similar spectra. Inlets show dendrograms of the bisecting k-means clustering demonstrating the overall number of clusters (color code), the number of "Spectra" in each cluster (integers), and the correlation distance ("Distance") between the clusters (decimals). Scale bars 2 cm.

area of interest to sections around the lymph node, that is clearly visible to the eye in iWAT. In a second step, we measured four sections of a single iWAT, spanning a range of ≈280 µm in a single run, to check for similarity of these sections (**Figure 1**A). Sections were examined by spatial segmentation of the spectra. The resulting segmentation map demonstrated a high similarity between the iWAT sections of a single mouse (Figure 1A). This observation was consolidated in two other 129S6/SvEvTac mice (Figure 1 B,C). These results demonstrate that no general methodological bias was introduced by our sectioning protocol, substantiating the comparability and reproducibility of sections in a defined region of iWAT. Additionally, the segmentation of regional spectra confirmed the heterogeneity within one iWAT section (Figure 1A–C), indicating regional specificity of lipid species.

3.2. Identification and Annotation of Region-specific *m/z* Intervals

After demonstrating the reliability of our MALDI-MSI approach, we asked the question of whether the spatial differences in the lipid composition correspond to specific functional regions within iWAT (Figure 1). Since several lipids are associated with cold induced NST on a whole tissue level,[7,8,21,22] we investigated, whether these changes of the lipidome observed upon cold stimulation appear ubiquitously in iWAT or are associated with clusters of thermogenic adipocytes. Therefore, we combined the MALDI-MSI data with IHC staining of UCP1, the major marker of brite adipocytes, and high-resolution LC-MS/MS (**Figure 2**A), to validate the findings of the MALDI-MSI on a global level. Staining of UCP1 in iWAT of cold acclimatized mice (129S6/SvEvTac) demonstrated the expected cluster of UCP1-expressing cells around the lymph node (Figure 2B, additional mouse examples, Figures S1 and S2A, Supporting Information).[14] As seen before (Figure 1), similar spectra clustered in specific regions and could be expanded until one cluster matched the UCP1 expression pattern (Figure 2B,C, additional mouse examples, Figures S1 and S2A,B, Supporting Information). To identify which *m/z* intervals discriminated between the regions overlapping with UCP1 expression (UCP1-positive) and those without overlap (UCP1-negative), we performed ROC-analysis between these two regions (Figure 2D, additional mouse examples Figures S1 and S2C, Supporting Information) in a total of $n = 8$ sections (3 mice with 2–4 sections). For each mouse, a mean area under the ROC curve (AUC_{ROC}) of ≥0.75 was considered characteristic for UCP1-positive regions, a mean AUC_{ROC} of ≤0.25 for the UCP1-negative regions, and a mean AUC_{ROC} between 0.45 and 0.55 to be not characteristic for any of the two regions. Using this approach,

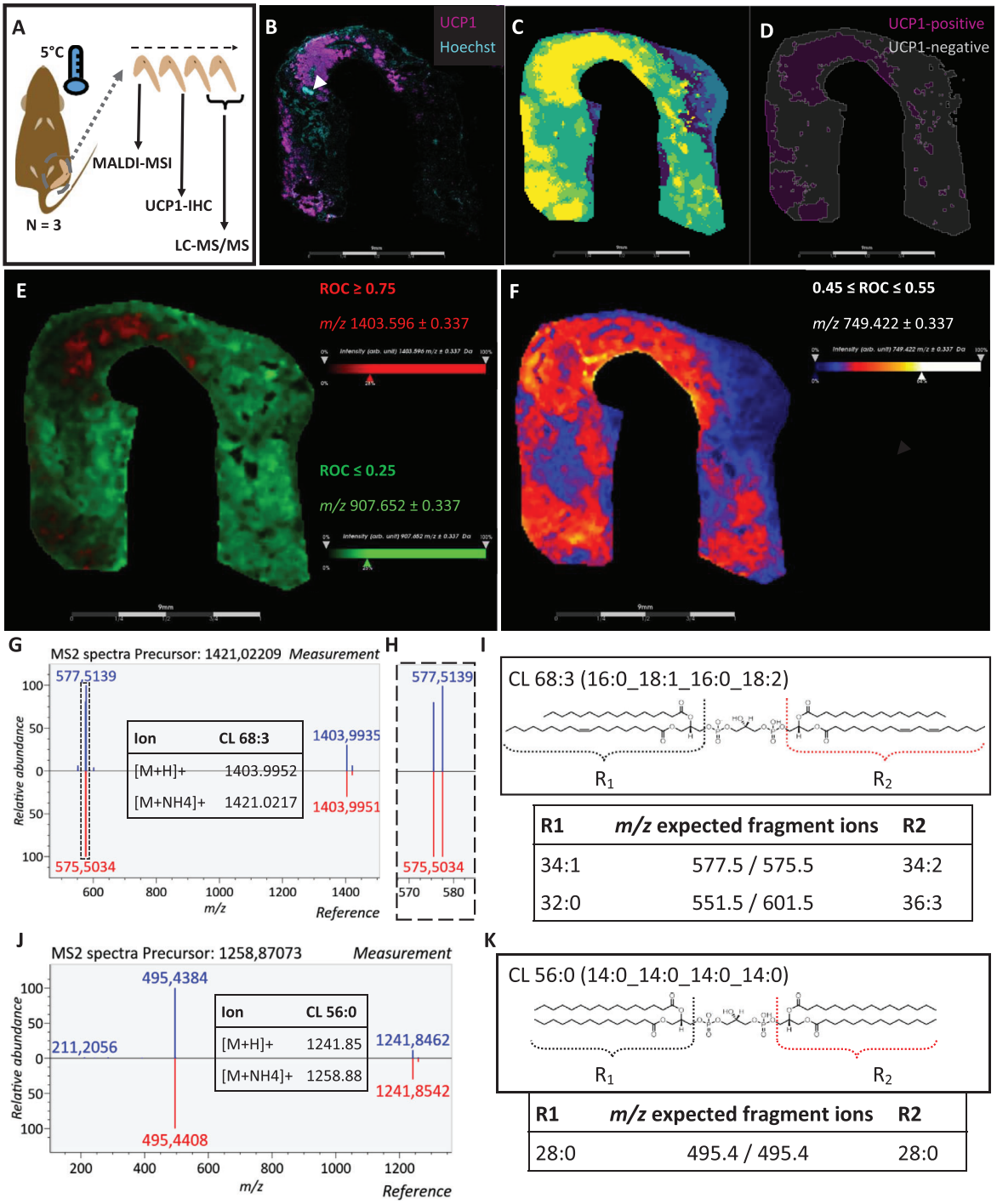

Figure 2. Identification and validation of region-specific lipid species. A) Overview of the experimental setup. 129S6/SvEvTac mice are housed at 5 °C for 1 week. iWAT is dissected (gray dashed circle). Four consecutive sections are prepared, the first used for MALDI-MSI, the second for IHC staining of UCP1, and the last two for LC-MS/MS analysis. B) IHC of iWAT stained for Ucp1 (magenta) and Hoechst (cyan). White arrowhead indicating the position of the lymph node. C) Segmentation map derived from spatial segmentation by bisecting k-means of the MALDI-data. Identical to Figure 1, identical colors indicate similar spectra. Clusters are expanded to several levels to match the Ucp1 pattern in B. D) Ucp1-pos (magenta) and Ucp1-neg (gray) adipose tissue regions assigned based on the segmentation used for ROC-analysis. E) MALDI images of two examples m/z intervals identified to be specific for the Ucp1-negative (green, $AUC_{ROC} \leq 0.25$) and Ucp1-positive (red, $AUC_{ROC} \geq 0.75$) regions depicted in (D). F) MALDI image of one example m/z interval not specific for any of the two regions assigned in (D) ($0.45 \leq AUC_{ROC} \leq 0.55$). G) MS2 spectra used to validate the region-specific m/z intervals exemplified on m/z 1403.596. Inlet shows the theoretical molecular masses of two different ions for CL 68:3 annotated by LIPID MAPS Structure database search. H) Detailed view of MS2 spectra of the m/z interval indicated by the dashed box in (G). I) Structure of CL 68:3 and fragments based on different acyl chain composition. J) MS2 spectra of a commercial CL standard (CL 56:0). K) Structure of CL 56:0 and fragments based on acyl chain composition.

Table 1. Overview of *m/z* intervals associated with UCP1-positive regions.

	MALDI		LIPID MAPS				LC-MS/MS			
	m/z	AUC_{ROC}	Match mass	Delta	Name	Formula	Ion	RT [min]	Measured mass	Delta [mDa]
1	1404.608	0.812	1404.8461	.2381	Hex(5)-Cer 38:1;O2	C68H125NO28				
2	1403.596	0.848	1403.9952	.3992	CL 68:3	C77H144O17P2	NH4+	19.7	1424.02051	1.22
3	1401.572	0.823	1401.8464	.2744	Hex(3)-HexNAc-Fuc-Cer 36:1;O2	C68H124N2O27				
			1401.9795	.4075	CL 68:4	C77H142O17P2	NH4+	19.3	1418.99646	9.64
4	1400.560	0.766	1400.826	.2660	Hex(2)-HexNAc-NeuGc-Cer 36:1;O2	C67H121N3O27				
5	1373.570	0.759	1373.8151	.2451	Hex(3)-HexNAc-Fuc-Cer 34:1;O2	C66H120N2O27				
6	619.195	0.818	619.2878	.0928	LPI 20:5	C29H47O12P				
			619.3606	.1656	PA 28:3;O2	C31H55O10P				
			619.3841	.1891	ST 35:5;O9	C35H54O9				
			619.4333	.2383	PA 30:1	C33H63O8P				
			619.4446	.2496	EPC 30:2;O3	C32H63N2O7P				
			619.4697	.2747	PA O-31:1	C34H67O7P				
			619.5296	.3346	DG 36:3	C39H70O5	NH4+	15.4	636.55463	1.58
			619.5449	.3499	CE 16:3	C43H70O2				
			619.6388	.4438	WE 42:1	C42H82O2				
7	618.183	0.853	618.3402	.1572	PE 25:4;O2	C30H52NO10P				
			618.4857	.3027	CerP 34:1;O2	C34H68NO6P				
8	617.171	0.848	617.4177	.2467	PA 30:2	C33H61O8P				
			617.4541	.2831	PA O-31:2	C34H65O7P				
			617.5139	.3429	DG 36:4	C39H68O5	NH4+	15	634.53876	1.77
			617.5503	.3793	DG O-37:4	C40H72O4				
9	615.146	0.759	615.3316	.1856	TG 35:13;O	C38H46O7				
			615.3504	.2044	LPI 19:0	C28H55O12P				
			615.3868	.2408	LPI O-20:0	C29H59O11P				
			615.402	.2560	PA 30:3	C33H59O8P				
			615.4983	.3523	DG 36:5	C39H66O5	NH4+	13.95	632.52106	3.84
10	571.287	0.815	571.2878	.0008	LPI 16:1	C25H47O12P				
11	570.275	0.841	570.2826	.0076	LPS 22:6	C28H44NO9P				
			570.3554	.0804	LPC 22:5	C30H52NO7P				
			570.3765	.1015	LPS O-21:0;O	C27H56NO9P				
			570.5092	.2342	Cer 34:1;O4	C34H67NO5				
			570.5456	.2706	Cer 35:0;O3	C35H71NO4				
12	569.263	0.837	569.3085	.0455	PG 20:1;O	C26H49O11P				
			569.332	.0690	ST 24:1;O4;GlcA	C30H48O10				
			569.3813	.1183	LPG 22:0	C28H57O9P				
			569.5139	.2509	DG 32:0	C35H68O5	NH4+	16.2	589.534	6.53
			569.5292	.2662	CE 12:0	C39H68O2				
13	567.239	0.757	567.2929	.0539	PA 23:2;O3	C26H47O11P				
			567.3528	.1138	ST 31:3;O9	C31H50O9				
			567.3656	.1266	LPG 22:1	C28H55O9P				
			567.4983	.2593	DG 32:1	C35H66O5	NH4+	15.2	584.52185	3.05
			567.5347	.2957	FAHFA 36:1;O	C36H70O4				
			567.5711	.3321	FA 37:0;O	C37H74O3				
14	559.142	0.812	559.2538	.1118	ST 30:8;O10	C30H38O10				
			559.2878	.1458	LPI 15:0	C24H47O12P				
			559.3242	.1822	LPI O-16:0	C25H51O11P				

(*Continued*)

Table 1. (Continued).

	MALDI		LIPID MAPS				LC-MS/MS			
	m/z	AUC_{ROC}	Match mass	Delta	Name	Formula	Ion	RT [min]	Measured mass	Delta [mDa]
			559.3265	.1845	ST 32:6;O8	C32H46O8				
			559.4357	.2937	DG 32:5	C35H58O5				
			559.4721	.3301	FAHFA 36:5;O	C36H62O4				
			559.5449	.4029	FA 38:3	C38H70O2				
			559.5449	.4029	WE 38:3	C38H70O2				
15	558.130	0.832	558.319	.1890	PC 20:4	C28H48NO8P				
			558.3459	.2159	ST 27:1;O5;T	C29H51NO7S				
			558.3554	.2254	LPC 21:4	C29H52NO7P				
16	557.117	0.759	557.2381	.1211	ST 30:9;O10	C30H36O10				
			557.2721	.1551	LPI 15:1	C24H45O12P				
			557.2874	.1704	LPG 22:6	C28H45O9P				
			557.3085	.1915	LPI O-16:1	C25H49O11P				
			557.3109	.1939	ST 32:7;O8	C32H44O8				
			557.5292	.4122	FA 38:4	C38H68O2				
17	511.234	0.846	511.2667	.0327	PA 20:1;O2	C23H43O10P				
			511.2902	.0562	FA 27:6;O7	C27H42O9				
			511.2902	.0562	MGMG 18:5	C27H42O9				
			511.303	.0690	LPG 18:1	C24H47O9P				
			511.3265	.0925	ST 28:2;O8	C28H46O8				
			511.4357	.2017	DG 28:1	C31H58O5	NH4+	8.8	528.46045	1.83
			511.4721	.2381	FAHFA 32:1;O	C32H62O4				
			511.4721	.2381	FA 32:1;O2	C32H62O4				
			511.5085	.2745	FA 33:0;O	C33H66O3				
18	511.909	0.802	512.2619	.3529	PS 16:0	C22H42NO10P				
			512.2983	.3893	LPS O-17:1;O	C23H46NO9P				
			512.2983	.3893	LPS 17:0	C23H46NO9P				
			511.5085	.4005	FA 33:0;O	C33H66O3				
			512.3347	.4257	LPS O-18:0	C24H50NO8P				
			511.4721	.4369	FAHFA 32:1;O	C32H62O4				
			511.4721	.4369	FA 32:1;O2	C32H62O4				
			512.3711	.4621	LPC O-17:0;O	C25H54NO7P				
			512.3711	.4621	LPE O-20:0;O	C25H54NO7P				
			511.4357	.4733	DG 28:1	C31H58O5	NH4+	12.8	528.46045	1.83
19	498.076	0.767	498.2826	.2066	LPS 16:0	C22H44NO9P				
			498.2826	.2066	LPS O-16:1;O	C22H44NO9P				
			498.3554	.2794	LPE O-19:0;O	C24H52NO7P				
			498.4881	.4121	Cer 31:0;O2	C31H63NO3				
20	485.931	0.760	486.2826	.3516	LPS O-15:0;O	C21H44NO9P				
			485.4928	.4382	FOH 31:0;O2	C31H64O3				
			485.4564	.4746	FA 30:0;O2	C30H60O4				
21	1375.594	0.791	No HIT							
22	1374.582	0.798	No HIT							
23	1402.584	0.859	No HIT							
24	616.158	0.816	No HIT							

m/z intervals associated with UCP1-negative regions by MALDI-MSI (*m/z*), based on their mean area under the ROC curve (AUC_{ROC}) and their matches to the LIPID MAPS structure database bulk search (mass, delta, name, and formula). If applicable the ion, retention time (RT), exact MS1 mass (measured mass), and delta to the matched reference mass are given for lipids that could be identified in the LC-MS/MS data by exact mass measurement and database hits for their respective MS2 fragmentation (gray highlights).

Table 2. Overview of *m/z* intervals associated with UCP1-negative regions.

	MALDI		LIPID MAPS				LC/MS			
	m/z	AUC_{ROC}	Match mass	Delta	Name	Formula	Ion	RT [min]	Measured mass	Delta [mDa]
1	472.436	0.76	472.3996	0.0364	CAR 20:0;O	C27H53NO5				
			472.3421	0.0939	CAR 22:6	C29H45NO4				
2	519.331	0.781	519.3316	0.0006	ST 30:4;O7	C30H46O7				
			519.4044	0.0734	ST 32:2;O5	C32H54O5				
			519.4408	0.1098	FAHFA 33:4;O	C33H58O4				
			519.5136	0.1826	FA 35:2	C35H66O2				
3	637.413	0.751	637.4075	0.0055	PG 26:1	C32H61O10P				
			637.3711	0.0419	PA 28:2;O3	C31H57O11P				
			637.4826	0.0696	DG 38:8	C41H64O5	Na+	16.21	659.46533	0.73
			637.3347	0.0783	PG 24:3;O2	C30H53O12P				
			637.5554	0.1424	DG dO-40:8	C43H72O3				
			637.5765	0.1635	DG 37:1	C40H76O5				
			637.5918	0.1788	CE 17:1	C44H76O2				
			637.6493	0.2363	FA 42:0;O	C42H84O3				
4	672.838	0.767	672.5409	0.2971	HexCer 32:1;O2	C38H73NO8				
			672.4599	0.3781	PE 31:3	C36H66NO8P				
5	679.248	0.789	679.3453	0.0973	PG 26:4;O3	C32H55O13P				
			679.3688	0.1208	ST 30:5;O7;Hex	C36H54O12				
			679.4333	0.1853	PA 35:6	C38H63O8P				
			679.4545	0.2065	PG 29:1	C35H67O10P				
			679.4697	0.2217	PA O-36:6	C39H67O7P				
			679.4908	0.2428	PG O-30:1	C36H71O9P				
			679.5871	0.3391	TG 39:1	C42H78O6				
			679.6235	0.3755	DG 40:1	C43H82O5				
			679.6388	0.3908	CE 20:1	C47H82O2				
			679.6963	0.4483	FA 45:0;O	C45H90O3				
6	680.26	0.76	680.3406	0.0806	PS 25:3;O3	C31H54NO13P				
			680.4133	0.1533	PE 28:2;O3	C33H62NO11P				
			680.4497	0.1897	PS 28:0	C34H66NO10P				
			680.4861	0.2261	PS O-29:0	C35H70NO9P				
			680.4861	0.2261	LPS O-29:1;O	C35H70NO9P				
			680.6551	0.3951	Cer 43:1;O3	C43H85NO4				
			680.6915	0.4315	Cer 44:0;O2	C44H89NO3				
7	734.578	0.772	734.5694	0.0086	PE 35:0	C40H80NO8P				
			734.5694	0.0086	PC 32:0	C40H80NO8P	H+	14.56	734.56848	0.92
			734.6058	0.0278	PC O-33:0	C41H84NO7P				
			734.6058	0.0278	PE O-36:0	C41H84NO7P				
			734.533	0.045	PS O-33:1	C39H76NO9P				
			734.4967	0.0813	PS 32:1	C38H72NO10P				
			734.4755	0.1025	PE 36:7	C41H68NO8P				
			734.4239	0.1541	PS 30:3;O2	C36H64NO12P				
			734.7385	0.1605	Cer 48:1;O2	C48H95NO3				
8	851.648	0.797	851.6008	0.0472	PI O-36:1	C45H87O12P				
			851.5913	0.0567	SQDG 36:0	C45H86O12S				
			851.7123	0.0643	TG 52:6	C55H94O6	NH4+	18.52	868.73773	1.16
			851.5797	0.0683	PG 42:6	C48H83O10P				
			851.5644	0.0836	PI 35:1	C44H83O13P				

(*Continued*)

Table 2. (Continued).

	MALDI		LIPID MAPS				LC/MS			
	m/z	AUC_{ROC}	Match mass	Delta	Name	Formula	Ion	RT [min]	Measured mass	Delta [mDa]
			851.4705	0.1775	PI 36:8	C45H71O13P				
			852.1436	0.4956	CoA 4:1;O	C25H40N7O18P3S				
9	852.66	0.761	852.6477	0.0123	PE 44:4	C49H90NO8P				
			852.6477	0.0123	PC 41:4	C49H90NO8P				
			852.6841	0.0241	PC O-42:4	C50H94NO7P				
			852.6113	0.0487	PS O-42:5	C48H86NO9P				
			852.5865	0.0735	SHexCer 38:1;O3	C44H85NO12S				
			852.5749	0.0851	PS 41:5	C47H82NO10P				
			852.5538	0.1062	PC 42:11	C50H78NO8P				
			852.8378	0.1778	Cer 54:0;O4	C54H109NO5				
			852.18	0.48	CoA 5:0	C26H44N7O17P3S				
10	853.672	0.791	853.6164	0.0556	PI O-36:0	C45H89O12P				
			853.728	0.056	TG 52:5	C55H96O6	NH4+	18.52	870.74457	9.95
			853.5953	0.0767	PG 42:5	C48H85O10P				
			853.5801	0.0919	PI 35:0	C44H85O13P				
			853.5613	0.1107	TG 51:14;O2	C54H76O8				
			853.4862	0.1858	PI 36:7	C45H73O13P				
			854.1229	0.4509	CoA 3:1;O2	C24H38N7O19P3S				
			854.1593	0.4873	CoA 4:0;O	C25H42N7O18P3S				
11	854.684	0.784	854.6997	0.0157	PC O-42:3	C50H96NO7P				
			854.6633	0.0207	PC 41:3	C49H92NO8P				
			854.6633	0.0207	PE 44:3	C49H92NO8P				
			854.6269	0.0571	PS O-42:4	C48H88NO9P				
			854.6117	0.0723	IPC 38:0;O3	C44H88NO12P				
			854.5906	0.0934	PS 41:4	C47H84NO10P				
			854.5694	0.1146	PC 42:10	C50H80NO8P	H+	11.6	854.5672	2.2
			854.4967	0.1873	PS 42:11	C48H72NO10P				
12	855.696	0.766	855.7436	0.0476	TG 52:4	C55H98O6	NH4+	18.96	872.75848	11.72
			855.611	0.085	PG 42:4	C48H87O10P				
			855.5018	0.1942	PI 36:6	C45H75O13P				
13	875.601	0.79	875.6008	0.0002	PI O-38:3	C47H87O12P				
			875.5797	0.0213	PG 44:8	C50H83O10P				
			875.5644	0.0366	PI 37:3	C46H83O13P				
			875.5456	0.0554	TG 53:17;O2	C56H74O8				
			875.6736	0.0726	PG 43:1	C49H95O10P				
			875.7123	0.1113	TG 54:8	C57H94O6	NH4+	18.29	892.72992	8.97
			875.8062	0.2052	TG 53:1	C56H106O6	NH4+	20.96	892.83044	2.38
14	876.951	0.76	876.6688	0.2822	PS 42:0	C48H94NO10P				
			876.6477	0.3033	PC 43:6	C51H90NO8P				
15	877.626	0.812	877.6164	0.0096	PI O-38:2	C47H89O12P				
			877.6528	0.0268	SLBPA 42:0	C48H93O11P				
			877.5953	0.0307	PG 44:7	C50H85O10P				
			877.5801	0.0459	PI 37:2	C46H85O13P				
			877.6892	0.0632	PG 43:0	C49H97O10P				
			877.728	0.102	TG 54:7	C57H96O6	NH4+	18.56	894.75409	0.43
			877.4862	0.1398	PI 38:9	C47H73O13P				
			877.8219	0.1959	TG 53:0	C56H108O6	NH4+	21.27	894.83875	9.64

(*Continued*)

Table 2. (Continued).

	MALDI		LIPID MAPS				LC/MS			
	m/z	AUC_{ROC}	Match mass	Delta	Name	Formula	Ion	RT [min]	Measured mass	Delta [mDa]
			877.8582	0.2322	FA 57:1;O3	C57H112O5				
			878.1229	0.4969	CoA 5:3;O2	C26H38N7O19P3S				
16	878.638	0.818	878.5906	0.0474	PS 43:6	C49H84NO10P				
			878.6997	0.0617	PC O-44:5	C52H96NO7P				
			878.5694	0.0686	PC 44:12	C52H80NO8P	H+	11.17	878.55914	10.26
			878.1957	0.4423	CoA 7:1	C28H46N7O17P3S				
			878.1593	0.4787	CoA 6:2;O	C27H42N7O18P3S				
17	879.65	0.805	879.6321	0.0179	PI O-38:1	C47H91O12P				
			879.611	0.039	PG 44:6	C50H87O10P				
			879.5957	0.0543	PI 37:1	C46H87O13P				
			879.5769	0.0731	TG 53:15;O2	C56H78O8				
			879.7436	0.0936	TG 54:6	C57H98O6	NH4+	20.92	896.76385	6.35
			879.5018	0.1482	PI 38:8	C47H75O13P				
			880.1385	0.4885	CoA 5:2;O2	C26H40N7O19P3S				
18	880.662	0.81	880.679	0.017	PC 43:4	C51H94NO8P				
			880.6178	0.0442	SHexCer 40:1;O3	C46H89NO12S				
			880.7154	0.0534	PC O-44:4	C52H98NO7P				
			880.5123	0.1497	PS 44:12	C50H74NO10P				
			880.2113	0.4507	CoA 7:0	C28H48N7O17P3S				
			880.1749	0.4871	CoA 6:1;O	C27H44N7O18P3S				
19	881.674	0.793	881.6477	0.0263	PI O-38:0	C47H93O12P				
			881.6266	0.0474	PG 44:5	C50H89O10P				
			881.6114	0.0626	PI 37:0	C46H89O13P				
			881.5926	0.0814	TG 53:14;O2	C56H80O8				
			881.7593	0.0853	TG 54:5	C57H100O6	NH4+	2013	898.78156	4.27
			881.5175	0.1565	PI 38:7	C47H77O13P				
			882.1542	0.4802	CoA 5:1;O2	C26H42N7O19P3S				
20	882.686	0.779	882.643	0.043	IPC 40:0;O3	C46H92NO12P				
			882.731	0.045	PC O-44:3	C52H100NO7P				
			882.6219	0.0641	PS 43:4	C49H88NO10P				
			882.6007	0.0853	PC 44:10	C52H84NO8P				
			882.1906	0.4954	CoA 6:0;O	C27H46N7O18P3S				
21	901.579	0.784	901.5801	0.0011	PI 39:4	C48H85O13P				
			901.6164	0.0374	PI O-40:4	C49H89O12P				
			901.6552	0.0762	TG 54:11;O2	C57H88O8	NH4+	18.3	918.66998	11.72
			901.728	0.149	TG 56:9	C59H96O6	NH4+	18.44	918.74487	9.65
			901.8219	0.2429	TG 55:2	C58H108O6	NH4+	20.88	918.84668	1.71
			901.931	0.352	FA 61:1;O	C61H120O3				
22	902.591	0.774	902.6845	0.0935	PS 44:1	C50H96NO10P				
			902.7572	0.1662	PC 44:0	C52H104NO8P				
			902.8899	0.2989	ACer 59:1;O2	C59H115NO4				
23	903.604	0.796	903.5957	0.0083	PI 39:3	C48H87O13P				
			903.6321	0.0281	PI O-40:3	C49H91O12P				
			903.5018	0.1022	PI 40:10	C49H75O13P				
			903.7436	0.1396	TG 56:8	C59H98O6	NH4+	19.07	920.76611	4.09
			903.8375	0.2335	TG 55:1	C58H110O6	NH4+	21.3	920.85712	6.95
24	904.616	0.786	904.7001	0.0841	PS 44:0	C50H98NO10P				

(*Continued*)

Table 2. (Continued).

	MALDI		LIPID MAPS				LC/MS			
	m/z	AUC_{ROC}	Match mass	Delta	Name	Formula	Ion	RT [min]	Measured mass	Delta [mDa]
25	905.628	0.8	905.6114	0.0166	PI 39:2	C48H89O13P				
			905.6477	0.0197	PI O-40:2	C49H93O12P				
			905.5175	0.1105	PI 40:9	C49H77O13P				
			905.7593	0.1313	TG 56:7	C59H100O6	NH4+	19.23	922.78302	2.81
			905.8532	0.2252	TG 55:0	C58H112O6	NH4+	21.52	922.87195	7.75
			905.8895	0.2615	FA 59:1;O3	C59H116O5				
26	906.64	0.793	906.6335	0.0065	SHexCer 42:2;O3	C48H91NO12S				
27	907.652	0.786	907.6634	0.0114	PI O-40:1	C49H95O12P				
			907.627	0.025	PI 39:1	C48H91O13P				
			907.5331	0.1189	PI 40:8	C49H79O13P				
			907.7749	0.1229	TG 56:6	C59H102O6	NH4+	19.61	924.79584	5.67
28	908.664	0.756	908.6491	0.0149	SHexCer 42:1;O3	C48H93NO12S				
			908.2426	0.4214	CoA 9:0	C30H52N7O17P3S				
			908.2062	0.4578	CoA 8:1;O	C29H48N7O18P3S				
			908.1698	0.4942	CoA 7:2;O2	C28H44N7O19P3S				

m/z intervals associated with UCP1-negative regions by MALDI-MSI (*m/z*), based on their mean area under the ROC curve (AUC_{ROC}) and their matches to the LIPID MAPS structure database bulk search (mass, delta, name, and formula). If applicable the ion, retention time (RT), exact MS1 mass (measured mass), and delta to the matched reference mass are given for lipids that could be identified in the LC-MS/MS data by exact mass measurement and database hits for their respective MS2 fragmentation (gray highlights).

we identified 24 *m/z* intervals associated with UCP1 expression (**Table 1**), 28 *m/z* intervals to UCP1-negative regions (**Table 2**), and 63 *m/z* intervals not specific for any of the two regions (**Table 3**). Visual inspection of the *m/z* intervals confirmed the discrimination potential of our approach (Figure 2E, additional mouse examples Figures S1 and S2D, Supporting Information). Within the set of *m/z* intervals not discriminating between the regions of interest, we identified some to be present ubiquitously (e.g., *m/z* 749.422, Figure 2F), and some to be associated with the lymph node (e.g., *m/z* 774.388, Figures S1 and S2F, Supporting Information). These *m/z* intervals were annotated to potential lipid species utilizing the bulk search option in the LMSD. In 8 instances no matching $[M+H]^+$ ion could be assigned to the entered *m/z* interval, resulting in 20 and 28 annotated *m/z* intervals for the UCP1-positive (Table 1) and UCP1-negative (Table 2) regions, respectively. Of the non-discriminating *m/z* intervals, 59 could be annotated to potential lipid species. Due to the broad mass tolerance (±0.5 Da) of the MALDI-measurement, we received 1–14 potential annotations for each *m/z* interval, corresponding to a variety of different lipid classes (Tables 1–3).

3.3. Validation of Annotated Lipid Species by High-Resolution LC-MS/MS

To limit the number of possible lipids per *m/z* interval we validated the presence of the lipids in our LC-MS/MS dataset generated on the third and fourth consecutive section of each MALDI sample. The annotated candidates identified by MALD-MSI were validated on a global level by searching for their LMSD annotated metabolite name in the LC-MS/MS dataset, considering their exact mass and their respective MS2 fragmentation pattern (Figure 2G,H). For example, CL demonstrate a characteristic fragmentation pattern where the diacylglyceride group is cleaved of the phosphatic backbone which can be used for the annotation of the correct carbon and double bond number of the diacyl side chains indicating that CL 68:3 consists of a C 34:1 and a C34:2 diacyl chain (Figure 2I). The general fragmentation pattern of CL was confirmed by analysis of a commercially available CL standard (CL 56:0) (Figure 2 J,K). Based on this approach we could confirm the presence of 8 of the annotated lipid species for the UCP1-positive and 21 for the UCP1-negative region on a global level, respectively (Tables 1 and 2). Concerning the UCP1-negative region, these were primarily triacylglycerols (TG), as well as diacylglycerophosphocholines (PC), and diacylglycerols (DG). The UCP1-positive regions were exclusively represented by DG and the two cardiolipins CL 68:3 and CL 68:4. This pattern supports our approach as TG is the main storage lipid, while CL is associated with thermogenic function in iWAT[8] and like UCP1 constitutes mitochondrial markers, almost exclusively present in mitochondrial membranes. In summary, the combined MALDI-MSI, IHC, LC-MS/MS approach allowed us to identify region-specific lipids linked to the thermogenic function of UCP1 expressing brite adipocytes.

3.4. CL 68:3 and CL 68:4 are Upregulated by Cold Independent of UCP1

We identified the cardiolipin species CL 68:3 and CL 68:4 to be associated with UCP1 expression in iWAT of cold acclimatized

Table 3. Overview of *m/z* intervals not discriminative between UCP1-positive and UCP1-negative regions.

	MALDI		LIPID MAPS				LC-MS/MS			
	m/z	AUC_{ROC}	Match mass	Delta	Name	Formula	Ion	RT [min]	Measured mass	Delta [mDa]
1	303.747	0.53	303.2682	0.4788	ST 21:1;O	C21H34O				
			303.253	0.494	MG O-14:1;O	C17H34O4				
			303.253	0.494	FA 17:0;O2	C17H34O4				
2	407.997	0.478	408.2744	0.2774	NA 23:5;O4	C23H37NO5				
			408.3472	0.3502	NA 25:3;O2	C25H45NO3				
3	440.048	0.493	440.2772	0.2292	LPE O-15:1;O	C20H42NO7P				
			440.2772	0.2292	LPC 12:0	C20H42NO7P				
			440.2772	0.2292	LPE 15:0	C20H42NO7P				
			440.3135	0.2655	LPE O-16:0	C21H46NO6P				
			440.3159	0.2679	NA 28:8;O2	C28H41NO3				
			440.337	0.289	CAR 18:2;O	C25H45NO5				
4	441.06	0.521	441.2999	0.2399	ST 28:5;O4	C28H40O4				
			441.3363	0.2763	ST 29:4;O3	C29H44O3				
			441.3727	0.3127	FA 30:6	C30H48O2				
			441.3727	0.3127	ST 30:3;O2	C30H48O2				
			441.3938	0.3338	FA 27:1;O2	C27H52O4				
			441.3938	0.3338	FAHFA 27:1;O	C27H52O4				
			441.4091	0.3491	ST 31:2;O	C31H52O				
			441.4302	0.3702	FA 28:0;O	C28H56O3				
			441.4666	0.4066	FOH 29:0;O	C29H60O2				
5	442.072	0.478	442.22	0.148	LPS 12:0	C18H36NO9P				
			442.2928	0.2208	LPE O-15:0;O	C20H44NO7P				
			442.3316	0.2596	NA 28:7;O2	C28H43NO3				
			442.3527	0.2807	CAR 18:1;O	C25H47NO5				
			443.1734	0.0894	ST 21:3;O5;S	C21H30O8S				
6	443.084	0.497	443.2041	0.1201	PG 12:0	C18H35O10P				
			443.2404	0.1564	LPG 13:0	C19H39O9P				
			443.2428	0.1588	ST 26:6;O6	C26H34O6				
			443.2792	0.1952	ST 27:5;O5	C27H38O5				
			443.3003	0.2163	WE 24:3;O5	C24H42O7				
			443.352	0.268	ST 29:3;O3	C29H46O3				
			443.3884	0.3044	ST 30:2;O2	C30H50O2				
			443.3884	0.3044	FA 30:5	C30H50O2				
			444.3683	0.2723	CAR 18:0;O	C25H49NO5				
7	467.038	0.52	467.2639	0.2259	FA 25:6;O6	C25H38O8				
			467.2639	0.2259	ST 19:1;O2;GlcA	C25H38O8				
			467.2792	0.2412	ST 29:7;O5	C29H38O5				
			467.3132	0.2752	LPA 20:0	C23H47O7P				
			467.319	0.281	ST 27:1;O;S	C27H46O4S				
			467.3367	0.2987	ST 27:1;O6	C27H46O6				
			467.3731	0.3351	ST 28:0;O5	C28H50O5				
			467.4459	0.4079	FA 29:1;O	C30H58O3				
			467.4823	0.4443	WE 31:0	C31H62O2				
			467.4823	0.4443	FA 31:0	C31H62O2				
			467.5186	0.4806	FOH 32:0	C32H66O				
8	482.895	0.454	483.2506	0.3556	LPA 22:6	C25H39O7P				
			483.2589	0.3639	ST 19:1;O3;GlcA	C25H38O9				

(*Continued*)

Table 3. (Continued).

	MALDI		LIPID MAPS				LC-MS/MS			
	m/z	AUC_{ROC}	Match mass	Delta	Name	Formula	Ion	RT [min]	Measured mass	Delta [mDa]
			483.2717	0.3767	LPG 16:1	C22H43O9P				
			483.3139	0.4189	ST 27:1;O2;S	C27H46O5S				
			482.4568	0.4382	Cer 30:1;O2	C30H59NO3				
9	487.28	0.499	487.2819	0.0019	LPA 22:4	C25H43O7P				
			487.2902	0.0102	MGMG 16:3	C25H42O9				
			487.269	0.011	ST 28:6;O7	C28H38O7				
			487.3054	0.0254	ST 29:5;O6	C29H42O6				
10	495.377	0.503	495.3445	0.0325	LPA 22:0	C25H51O7P				
			495.3316	0.0454	ST 28:2;O7	C28H46O7				
			495.3105	0.0665	ST 31:7;O5	C31H42O5				
			495.2952	0.0818	ST 27:3;O8	C27H42O8				
			495.2717	0.1053	PA 20:1;O	C23H43O9P				
			495.2717	0.1053	LPG 17:2	C23H43O9P				
			495.5136	0.1366	FA 33:0	C33H66O2				
			495.5136	0.1366	WE 33:0	C33H66O2				
			495.5499	0.1729	FOH 34:0	C34H70O				
11	499.426	0.499	499.451	0.025	WE 34:5	C34H58O2				
			499.451	0.025	FA 34:5	C34H58O2				
			499.3394	0.0866	LPG O-18:0	C24H51O8P				
			499.3054	0.1206	ST 30:6;O6	C30H42O6				
			499.303	0.123	LPG 17:0	C23H47O9P				
			499.2724	0.1536	ST 26:2;O4;S	C26H42O7S				
			499.2667	0.1593	PG 16:0	C22H43O10P				
12	500.101	0.538	500.2772	0.1762	LPE 20:5	C25H42NO7P				
			500.2983	0.1973	LPS O-16:0;O	C22H46NO9P				
			500.304	0.203	ST 24:1;O4;T	C26H45NO6S				
13	502.125	0.498	502.2564	0.1314	PC 16:4	C24H40NO8P				
			502.2928	0.1678	LPE 20:4	C25H44NO7P	H+	2.53	502.29153	1.2
14	504.149	0.524	504.3085	0.1595	LPE 20:3	C25H46NO7P				
			504.4081	0.2591	NAT 26:0	C28H57NO4S				
			506.3241	0.1501	LPE 20:2	C25H48NO7P				
			506.3241	0.1501	LPC 17:2	C25H48NO7P				
			506.3605	0.1865	LPC O-18:2	C26H52NO6P				
			506.3605	0.1865	CerP 26:1;O2	C26H52NO6P				
			506.4568	0.2828	Cer 32:3;O2	C32H59NO3				
15	514.271	0.518	514.3139	0.0429	LPS O-17:0;O	C23H48NO9P				
16	515.283	0.528	515.3003	0.0173	ST 30:6;O7	C30H42O7				
			515.3037	0.0207	ST 27:1;O4;S	C27H46O7S				
17	522.368	0.486	522.3554	0.0126	PC O-18:1	C26H52NO7P				
			522.3554	0.0126	LPC 18:1	C26H52NO7P	H+	3.4	552.35437	1.04
			522.4517	0.0837	Cer 32:3;O3	C32H59NO4				
			522.2826	0.0854	LPS 18:2	C24H44NO9P				
			522.4881	0.1201	Cer 33:2;O2	C33H63NO3				
			522.5244	0.1564	Cer 34:1;O	C34H67NO2				
18	525.404	0.484	525.4513	0.0473	DG 29:1	C32H60O5	Na+	30.69	447.41901	14.28
			525.3551	0.0489	LPG O-20:1	C26H53O8P				
			525.4666	0.0626	WE 36:6	C36H60O2				

(*Continued*)

Table 3. (Continued).

	MALDI		LIPID MAPS				LC-MS/MS			
	m/z	AUC_{ROC}	Match mass	Delta	Name	Formula	Ion	RT [min]	Measured mass	Delta [mDa]
			525.4666	0.0626	FA 36:6	C36H60O2				
			525.4877	0.0837	FAHFA 33:1;O	C33H64O4				
			525.3187	0.0853	LPG 19:1	C25H49O9P				
			525.5241	0.1201	FA 34:0;O	C34H68O3				
			525.2823	0.1217	PA 21:1;O2	C24H45O10P				
19	526.079	0.488	526.2928	0.2138	LPE 22:6	C27H44NO7P				
			526.3139	0.2349	LPS 18:0	C24H48NO9P				
			526.3139	0.2349	LPS O-18:1;O	C24H48NO9P				
			526.3867	0.3077	LPE O-21:0;O	C26H56NO7P				
			526.483	0.404	Cer 32:1;O3	C32H63NO4				
			526.5194	0.4404	Cer 33:0;O2	C33H67NO3				
20	534.176	0.487	534.2826	0.1066	LPE 20:4;O2	C25H44NO9P				
			534.3554	0.1794	LPE 22:2	C27H52NO7P				
			534.3554	0.1794	LPC 19:2	C27H52NO7P				
			534.4881	0.3121	Cer 34:3;O2	C34H63NO3				
21	544.297	0.537	544.267	0.03	LPS 20:5	C26H42NO9P				
			544.3398	0.0428	LPC 20:4	C28H50NO7P	H+	2.44	544.3344	5.37
22	562.178	0.523	562.4231	0.2451	CerP 30:1;O2	C30H60NO6P				
			562.5194	0.3414	Cer 36:3;O2	C36H67NO3				
23	564.202	0.544	564.3296	0.1276	PE 22:2;O	C27H50NO9P				
			564.366	0.164	PC 20:1	C28H54NO8P				
			564.4024	0.2004	PC O-21:1	C29H58NO7P				
			564.4024	0.2004	LPE 24:1	C29H58NO7P				
			564.535	0.333	Cer 36:2;O2	C36H69NO3	H+	14.66	564.53223	2.74
24	623.918	0.54	623.5762	0.3419	CE 16:1	C43H74O2	NH4+	19.89	640.6145	11.78
			623.5609	0.3571	DG 36:1	C39H74O5	NH4+	16.99	640.586	1.52
			624.3143	0.3963	PS 22:2;O2	C28H50NO12P				
			623.5034	0.4146	DG O-38:8	C41H66O4				
			623.4881	0.4299	FOH 37:5;O6	C37H66O7				
			624.3507	0.4327	PE 24:2;O3	C29H54NO11P				
			624.3871	0.4691	PS 24:0	C30H58NO10P				
			624.3871	0.4691	PE 25:1;O2	C30H58NO10P				
25	625.942	0.483	625.5918	0.3502	CE 16:0	C43H76O2				
			625.5765	0.3655	DG 36:0	C39H76O5	Na+	19.23	647.54938	9.09
			625.4826	0.4594	DG 37:7	C40H64O5	Na+	15.63	647.46136	3.24
			626.4391	0.4971	LPS O-25:0;O	C31H64NO9P				
26	634.039	0.528	634.3351	0.2961	PE 25:4;O3	C30H52NO11P				
			634.3715	0.3325	PE 26:3;O2	C31H56NO10P				
			634.3715	0.3325	PC 23:3;O2	C31H56NO10P				
			634.4078	0.3688	PE 27:2;O	C32H60NO9P				
			634.4442	0.4052	PE 28:1	C33H64NO8P				
			634.4806	0.4416	CerP 34:1;O3	C34H68NO7P				
			634.4806	0.4416	PE O-29:1	C34H68NO7P				
			634.4806	0.4416	LPE O-29:2;O	C34H68NO7P				
			633.5452	0.4938	DG 37:3	C40H72O5				
27	647.197	0.457	647.3919	0.1949	PA 30:3;O2	C33H59O10P				
			647.4646	0.2676	PA 32:1	C35H67O8P				

(*Continued*)

Table 3. (Continued).

	MALDI		LIPID MAPS				LC-MS/MS			
	m/z	AUC_{ROC}	Match mass	Delta	Name	Formula	Ion	RT [min]	Measured mass	Delta [mDa]
			647.4759	0.2789	EPC 32:2;O3	C34H67N2O7P				
			647.501	0.304	PA O-33:1	C36H71O7P				
			647.5122	0.3152	EPC 33:1;O2	C35H71N2O6P				
			647.5122	0.3152	SM 30:1;O2	C35H71N2O6P				
			647.5609	0.3639	DG 38:3	C41H74O5	NH4+	16.23	664.58398	3.54
			647.5762	0.3792	CE 18:3	C45H74O2				
28	651.246	0.508	651.3504	0.1044	PG 25:3;O2	C31H55O12P				
			651.4232	0.1772	PG 27:1	C33H63O10P				
			651.4595	0.2135	PG O-28:1	C34H67O9P				
			651.4983	0.2523	DG 39:8	C42H66O5				
			651.5072	0.2612	EPC 32:0;O3	C34H71N2O7P				
			651.5347	0.2887	DG O-40:8	C43H70O4				
			651.5922	0.3462	DG 38:1	C41H78O5				
			651.6075	0.3615	CE 18:1	C45H78O2	NH4+	17.78	668.63171	2.26
			651.6286	0.3826	WD 42:1;O2	C42H82O4				
			651.665	0.419	FA 43:0;O	C43H86O3				
29	654.282	0.488	654.3249	0.0429	PS 23:2;O3	C29H52NO13P				
			654.6031	0.3211	Cer 40:1;O4	C40H79NO5				
			654.6395	0.3575	Cer 41:0;O3	C41H83NO4				
30	703.876	0.514	703.6388	0.2373	CE 22:3	C49H82O2				
			703.6235	0.2525	DG 42:3	C45H82O5				
			703.5748	0.3012	EPC 37:1;O2	C39H79N2O6P				
			703.5748	0.3012	SM 34:1;O2	C39H79N2O6P	H+	13.53	703.57416	0.73
			703.5636	0.3124	PA O-37:1	C40H79O7P				
			703.5385	0.3375	EPC 36:2;O3	C38H75N2O7P				
			703.5355	0.3405	MGDG 30:0	C39H74O10				
			703.5272	0.3488	PA 36:1	C39H75O8P				
			703.4545	0.4215	PG 31:3	C37H67O10P				
31	704.889	0.466	704.6915	0.1975	Cer 46:2;O2	C46H89NO3				
			704.5589	0.3301	PE O-34:1	C39H78NO7P				
			704.5589	0.3301	PC O-31:1	C39H78NO7P				
			704.5225	0.3665	PE 33:1	C38H74NO8P	H+	14.53	704.53235	9.83
			704.5225	0.3665	PC 30:1	C38H74NO8P	Na+	12.09	726.50067	3.72
			704.4861	0.4029	PS O-31:2	C37H70NO9P				
			704.4497	0.4393	PS 30:2	C36H66NO10P				
			704.4497	0.4393	PC 28:3;O2	C36H66NO10P				
			704.4133	0.4757	PE 30:4;O3	C35H62NO11P				
32	729.18	0.475	729.3457	0.1657	PI 23:2;O3	C32H57O16P				
			729.4701	0.2901	PG 33:4	C39H69O10P				
			729.5065	0.3265	PG O-34:4	C40H73O9P				
			729.5429	0.3629	PA 38:2	C41H77O8P				
			729.5511	0.3711	MGDG 32:1	C41H76O10				
			729.5541	0.3741	EPC 38:3;O3	C40H77N2O7P				
			729.5793	0.3993	PA O-39:2	C42H81O7P				
			729.5905	0.4105	SM 36:2;O2	C41H81N2O6P	H+	13.78	729.58661	3.91
			729.5905	0.4105	EPC 39:2;O2	C41H81N2O6P				
			729.6028	0.4228	TG 43:4	C46H80O6	NH4+	16.7	746.56885	0.55

(*Continued*)

Table 3. (Continued).

	MALDI		LIPID MAPS				LC-MS/MS			
	m/z	AUC_{ROC}	Match mass	Delta	Name	Formula	Ion	RT [min]	Measured mass	Delta [mDa]
			729.6391	0.4591	DG 44:4	C47H84O5				
33	749.422	0.542	749.3719	0.0501	LPIM1 17:0	C32H61O17P				
			749.5116	0.0896	PA 40:6	C43H73O8P				
			749.5327	0.1107	PG 34:1	C40H77O10P				
			749.5327	0.1107	LBPA 34:1	C40H77O10P				
			749.5691	0.1471	PG O-35:1	C41H81O9P				
			749.6654	0.2434	TG 44:1	C47H88O6	NH4+	18.96	766.68427	7.62
34	750.434	0.523	750.4188	0.0152	PS 30:3;O3	C36H64NO13P				
			750.5068	0.0728	PC 34:6	C42H72NO8P				
			750.5068	0.0728	PE 37:6	C42H72NO8P				
			750.528	0.094	PS 33:0	C39H76NO10P				
			750.5432	0.1092	PE O-38:6	C43H76NO7P				
			750.5643	0.1303	PS O-34:0	C40H80NO9P				
			750.7334	0.2994	Cer 48:1;O3	C48H95NO4				
			750.7698	0.3358	Cer 49:0;O2	C49H99NO3				
35	751.447	0.517	751.4392	0.0078	PI 28:2	C37H67O13P				
			751.5272	0.0802	PA 40:5	C43H75O8P				
			751.3664	0.0806	PI 26:4;O2	C35H59O15P				
			751.5484	0.1014	PG 34:0	C40H79O10P				
			751.5847	0.1377	PG O-35:0	C41H83O9P				
			751.681	0.234	TG 44:0	C47H90O6	NH4+	19.43	768.69922	8.36
36	752.459	0.524	752.4497	0.0093	PS 34:6	C40H66NO10P				
			752.5072	0.0482	IPC 32:1;O2	C38H74NO11P				
			752.5225	0.0635	PC 34:5	C42H74NO8P				
			752.5225	0.0635	PE 37:5	C42H74NO8P	H+	13.08	752.51648	6.04
			752.5589	0.0999	PE O-38:5	C43H78NO7P				
			752.6035	0.1445	HexCer 38:3;O2	C44H81NO8				
			752.7126	0.2536	Cer 47:1;O4	C47H93NO5				
			752.749	0.29	Cer 48:0;O3	C48H97NO4				
37	774.388	0.504	774.5068	0.1188	PC 36:8	C44H72NO8P	Na+	15.13	796.505	16.23
			774.5068	0.1188	PE 39:8	C44H72NO8P				
			774.528	0.14	PS 35:2	C41H76NO10P				
			774.5432	0.1552	PE O-40:8	C45H76NO7P				
			774.5643	0.1763	PS O-36:2	C42H80NO9P				
			774.5796	0.1916	PC dO-38:8	C46H80NO6P				
			774.5878	0.1998	DGCC 36:5	C46H79NO8				
			774.6007	0.2127	PE 38:1	C43H84NO8P				
			774.6007	0.2127	PC 35:1	C43H84NO8P	H+	15.26	774.60187	1.16
			774.609	0.221	HexCer 37:1;O4	C43H83NO10				
			774.6371	0.2491	PE O-39:1	C44H88NO7P				
			774.6371	0.2491	PC O-36:1	C44H88NO7P				
			774.6454	0.2574	HexCer 38:0;O3	C44H87NO9				
38	775.400	0.509	775.3876	0.0124	LPIM1 19:1	C34H63O17P				
			775.4392	0.0392	PI 30:4	C39H67O13P				
			775.4627	0.0627	MGDG 34:8;O2	C43H66O12				
			775.4908	0.0908	PG O-38:9	C44H71O9P				
			775.5272	0.1272	PA 42:7	C45H75O8P				

(*Continued*)

Table 3. (Continued).

	MALDI		LIPID MAPS				LC-MS/MS			
	m/z	AUC_{ROC}	Match mass	Delta	Name	Formula	Ion	RT [min]	Measured mass	Delta [mDa]
			775.5355	0.1355	MGDG 36:6	C45H74O10				
			775.5484	0.1484	PG 36:2	C42H79O10P	NH4+	13.73	792.5838	8.91
			775.5484	0.1484	LBPA 36:2	C42H79O10P				
			775.5847	0.1847	PG O-37:2	C43H83O9P				
			775.6211	0.2211	PA 41:0	C44H87O8P				
			775.6575	0.2575	PA O-42:0	C45H91O7P				
			775.6687	0.2687	SM 39:0;O2	C44H91N2O6P				
			775.681	0.281	TG 46:2	C49H90O6	NH4+	18.94	792.70148	6.1
39	786.534	0.544	786.528	0.006	PS 36:3	C42H76NO10P				
			786.5432	0.0092	PC O-38:9	C46H76NO7P				
			786.5068	0.0272	PE 40:9	C45H72NO8P				
			786.5643	0.0303	PS O-37:3	C43H80NO9P				
			786.6007	0.0667	PE 39:2	C44H84NO8P				
			786.6007	0.0667	PC 36:2	C44H84NO8P	H+	14.86	786.59955	1.16
			786.6371	0.1031	PC O-37:2	C45H88NO7P				
			786.6371	0.1031	PE O-40:2	C45H88NO7P				
			786.6454	0.1114	HexCer 39:1;O3	C45H87NO9				
			786.6817	0.1477	HexCer 40:0;O2	C46H91NO8				
40	792.269	0.505	792.481	0.212	PS 37:7	C43H70NO10P				
			792.5174	0.2484	PS O-38:7	C44H74NO9P				
			792.5538	0.2848	PE 40:6	C45H78NO8P	H+	14.43	792.55573	1.96
			792.5538	0.2848	PC 37:6	C45H78NO8P				
			792.5538	0.2848	PE O-40:7;O	C45H78NO8P				
			792.5749	0.3059	PS 36:0	C42H82NO10P				
			792.5902	0.3212	PC O-38:6	C46H82NO7P				
			792.6113	0.3423	PS O-37:0	C43H86NO9P				
			792.6841	0.4151	PE dO-40:0	C45H94NO7P				
41	794.293	0.468	794.4967	0.2037	PS 37:6	C43H72NO10P				
			794.533	0.24	PS O-38:6	C44H76NO9P				
			794.5694	0.2764	PE 40:5	C45H80NO8P	H+	15.13	794.56653	2.87
			794.5694	0.2764	PC 37:5	C45H80NO8P	Na+	14.14	816.54889	2.5
			794.6058	0.3128	PC O-38:5	C46H84NO7P	H+	14.17	794.60223	3.54
			794.7596	0.4666	Cer 50:1;O4	C50H99NO5				
42	796.318	0.529	796.5123	0.1943	PS 37:5	C43H74NO10P				
			796.5239	0.2059	SHexCer 34:1;O3	C40H77NO12S				
			796.5487	0.2307	PS O-38:5	C44H78NO9P				
			796.5851	0.2671	PE 40:4	C45H82NO8P				
			796.5851	0.2671	PC 37:4	C45H82NO8P				
			796.6215	0.3035	PC O-38:4	C46H86NO7P				
			796.6661	0.3481	HexCer 41:2;O2	C47H89NO8				
			796.7752	0.4572	Cer 50:0;O4	C50H101NO5				
43	797.33	0.537	797.4083	0.0783	PI 28:3;O3	C37H65O16P				
			797.5116	0.1816	PA 44:10	C47H73O8P				
			797.5175	0.1875	PI 31:0	C40H77O13P				
			797.5198	0.1898	MGDG 38:9	C47H72O10				
			797.5198	0.1898	FA 47:11;O8	C47H72O10				
			797.5327	0.2027	PG 38:5	C44H77O10P				

(*Continued*)

European Journal of Lipid Science and Technology
www.ejlst.com

Table 3. (Continued).

	MALDI		LIPID MAPS				LC-MS/MS			
	m/z	AUC_{ROC}	Match mass	Delta	Name	Formula	Ion	RT [min]	Measured mass	Delta [mDa]
			797.5538	0.2238	PI O-32:0	C41H81O12P				
			797.5562	0.2262	FA 48:10;O7	C48H76O9				
			797.6654	0.3354	TG 48:5	C51H88O6				
44	798.342	0.53	798.528	0.186	PS 37:4	C43H76NO10P				
			798.5491	0.2071	IPC 34:0;O3	C40H80NO12P				
			798.5643	0.2223	PS O-38:4	C44H80NO9P				
			798.5643	0.2223	PC 36:4;O	C44H80NO9P				
			798.6007	0.2587	PC 37:3	C45H84NO8P				
			798.6007	0.2587	PE 40:3	C45H84NO8P	H+	15.73	796.58105	4.03
			798.6371	0.2951	PC O-38:3	C46H88NO7P				
			798.6454	0.3034	HexCer 40:2;O3	C46H87NO9				
			798.6817	0.3397	HexCer 41:1;O2	C47H91NO8	H-H2O	17.17	780.6665	4.7
45	802.391	0.48	802.4654	0.0744	PS 38:9	C44H68NO10P				
			802.5381	0.1471	PC 38:8	C46H76NO8P	H+	15.89	802.55225	14.16
			802.5593	0.1683	PS 37:2	C43H80NO10P				
			802.5956	0.2046	PS O-38:2	C44H84NO9P				
			802.6109	0.2199	PC dO-40:8	C48H84NO6P				
			802.632	0.241	PE 40:1	C45H88NO8P				
			802.632	0.241	PC 37:1	C45H88NO8P	H+	15.85	802.62744	4.58
			802.6684	0.2774	PC O-38:1	C46H92NO7P	H+	15.83	802.65314	15.26
			802.6684	0.2774	PE O-41:1	C46H92NO7P				
46	803.403	0.542	803.4705	0.0675	PI 32:4	C41H71O13P				
			803.494	0.091	MGDG 36:8;O2	C45H70O12				
			803.5221	0.1191	PG dO-40:10;1	C46H75O9P				
			803.5585	0.1555	PA 44:7	C47H79O8P				
			803.5797	0.1767	PG 38:2	C44H83O10P				
			803.616	0.213	PG O-39:2	C45H87O9P				
			803.6524	0.2494	PA 43:0	C46H91O8P				
			803.7	0.297	SM 41:0;O2	C46H95N2O6P				
			803.7123	0.3093	TG 48:2	C51H94O6	NH4+	19.47	830.73541	3.48
47	818.247	0.513	818.4967	0.2497	PS 39:8	C45H72NO10P				
			818.5694	0.3224	PC 39:7	C47H80NO8P	Na+	9.79	840.57007	18.68
			818.5694	0.3224	PE 42:7	C47H80NO8P	H+	14.36	818.56311	6.29
			818.5906	0.3436	PS 38:1	C44H84NO10P	H+	11.19	840.57062	1.89
			818.6058	0.3588	PC O-40:7	C48H84NO7P	H+	13.71	818.5929	12.87
			818.6269	0.3799	PS O-39:1	C45H88NO9P				
			817.8371	0.4099	FA 55:1;O	C55H108O3				
			818.6633	0.4163	PE 41:0	C46H92NO8P				
			818.6633	0.4163	PC 38:0	C46H92NO8P				
			818.6633	0.4163	PE-NMe 40:0	C46H92NO8P				
			818.6716	0.4246	HexCer 40:0;O4	C46H91NO10				
			818.6997	0.4527	PE O-42:0	C47H96NO7P				
			818.6997	0.4527	PC O-39:0	C47H96NO7P	H+	15.83	818.69971	3.3
			818.7361	0.4891	PC dO-40:0	C48H100NO6P				
48	820.271	0.525	820.5123	0.2413	PS 39:7	C45H74NO10P				
			820.5487	0.2777	PS O-40:7	C46H78NO9P				
			820.5851	0.3141	PC 39:6	C47H82NO8P				

(*Continued*)

Table 3. (Continued).

	MALDI		LIPID MAPS				LC-MS/MS			
	m/z	AUC_{ROC}	Match mass	Delta	Name	Formula	Ion	RT [min]	Measured mass	Delta [mDa]
			820.5851	0.3141	PE 42:6	C47H82NO8P	H+	15.34	820.57391	11.17
			820.6062	0.3352	PS 38:0	C44H86NO10P				
			820.6215	0.3505	PC O-40:6	C48H86NO7P	H+	14.08	820.61121	10.31
			820.6426	0.3716	PS O-39:0	C45H90NO9P				
49	821.284	0.539	821.5175	0.2335	PI 33:2	C42H77O13P				
			821.5327	0.2487	PG 40:7	C46H77O10P				
			821.5538	0.2698	PI O-34:2	C43H81O12P				
			821.6266	0.3426	PG 39:0	C45H89O10P				
			821.663	0.379	PG O-40:0	C46H93O9P				
			821.6654	0.3814	TG 50:7	C53H88O6	NH4+	17.44	838.69379	1.9
			820.8116	0.4724	Cer 53:1;O3	C53H105NO4				
			821.7593	0.4753	TG 49:0	C52H100O6	NH4+	20.6	838.78217	3.66
50	822.633	0.499	822.6371	0.0041	PC O-40:5	C48H88NO7P				
			822.6007	0.0323	PC 39:5	C47H84NO8P				
			822.6007	0.0323	PE 42:5	C47H84NO8P				
			822.5643	0.0687	PS O-40:6	C46H80NO9P				
			822.528	0.105	PS 39:6	C45H76NO10P				
			822.7909	0.1579	Cer 52:1;O4	C52H103NO5				
			822.1331	0.4999	CoA 3:1	C24H38N7O17P3S				
51	828.369	0.522	828.481	0.112	PS 40:10	C46H70NO10P				
			828.5385	0.1695	PC 36:5;O3	C44H78NO11P				
			828.5538	0.1848	PC 40:9	C48H78NO8P	H+	11.06	828.54846	5.31
			828.5749	0.2059	PS 39:3	C45H82NO10P				
			828.6113	0.2423	PS O-40:3	C46H86NO9P				
			828.6477	0.2787	PC 39:2	C47H90NO8P				
			828.6477	0.2787	PE 42:2	C47H90NO8P				
			828.6841	0.3151	PC O-40:2	C48H94NO7P				
			828.6923	0.3233	HexCer 42:1;O3	C48H93NO9	H-H2O	17.4	810.67603	5.67
52	829.381	0.514	829.4862	0.1052	PI 34:5	C43H73O13P				
			829.499	0.118	PGP 34:1	C40H78O13P2				
			829.5097	0.1287	FA 47:11;O10	C47H72O12				
			829.5953	0.2143	PG 40:3	C46H85O10P				
			829.7157	0.3347	SM 43:1;O2	C48H97N2O6P	H+	17.82	829.70935	6.35
			829.728	0.347	TG 50:3	C53H96O6	NH4+	18.9	846.7442	10.32
53	830.393	0.453	830.4967	0.1037	PS 40:9	C46H72NO10P				
			830.5542	0.1612	PC 36:4;O3	C44H80NO11P				
			830.5694	0.1764	PC 40:8	C48H80NO8P	Na+	11.95	852.55157	0.18
			830.5906	0.1976	PS 39:2	C45H84NO10P				
			830.6269	0.2339	PS O-40:2	C46H88NO9P				
			830.6633	0.2703	PE 42:1	C47H92NO8P				
			830.6633	0.2703	PC 39:1	C47H92NO8P				
			830.6997	0.3067	PC O-40:1	C48H96NO7P				
54	845.237	0.488	845.5175	0.2805	PI 35:4	C44H77O13P				
			845.5327	0.2957	PG 42:9	C48H77O10P				
			845.5538	0.3168	PI O-36:4	C45H81O12P				
			845.6266	0.3896	PG 41:2	C47H89O10P				
			845.663	0.426	PG O-42:2	C48H93O9P				

(*Continued*)

Table 3. (Continued).

	MALDI		LIPID MAPS				LC-MS/MS			
	m/z	AUC_{ROC}	Match mass	Delta	Name	Formula	Ion	RT [min]	Measured mass	Delta [mDa]
			845.6654	0.4284	TG 52:9	C55H88O6	Na+	17.4	867.62848	18.8
55	846.25	0.512	846.6007	0.3507	PC 41:7	C49H84NO8P				
			846.6007	0.3507	PE 44:7	C49H84NO8P				
			846.6219	0.3719	PS 40:1	C46H88NO10P	H+	16.49	846.61298	8.91
			845.8684	0.3816	FA 57:1;O	C57H112O3				
			846.6371	0.3871	PC O-42:7	C50H88NO7P				
			846.6582	0.4082	PS O-41:1	C47H92NO9P				
			846.6946	0.4446	PE 43:0	C48H96NO8P				
			846.6946	0.4446	PC 40:0	C48H96NO8P				
			846.731	0.481	PC O-41:0	C49H100NO7P				
			845.7593	0.4907	TG 51:2	C54H100O6	NH4+	20.15	862.78339	2.44
56	862.106	0.46	861.7906	0.3154	TG 52:1	C55H104O6	NH4+	20.81	878.81641	0.67
			861.6967	0.4093	TG 53:8	C56H92O6	NH4+	18.63	894.72723	9.15
			861.6579	0.4481	PG 42:1	C48H93O10P				
			862.5593	0.4533	PS 42:7	C48H80NO10P				
57	863.118	0.52	862.6895	0.4285	PS O-42:0	C48H96NO9P				
			863.5644	0.4464	PI 36:2	C45H83O13P	NH4+	13.61	880.58563	5.37
			862.6532	0.4648	PS 41:0	C47H92NO10P				
			863.6008	0.4828	PI O-37:2	C46H87O12P				
			862.632	0.486	PC 42:6	C50H88NO8P				
			862.625	0.493	Hex2Cer 34:1;O2	C46H87NO13				
58	914.062	0.497	914.1593	0.0973	CoA 9:5;O	C30H42N7O18P3S				
			913.8219	0.2401	TG 56:3	C59H108O6	NH4+	18.32	930.83075	17.64
			913.728	0.334	TG 57:10	C60H96O6	Na+	20.03	935.71002	0.12
			913.5801	0.4819	PI 40:5	C49H85O13P				
59	955.222	0.454	955.5331	0.3111	PI 44:12	C53H79O13P				
			954.7885	0.4335	PC 48:2	C56H108NO8P				
60	444.096	0.508	No HIT							
61	506.174	0.511	No HIT							
62	913.05	0.457	No HIT							
63	915.074	0.487	No HIT							

m/z intervals associated with UCP1-negative regions by MALDI-MSI (*m/z*). based on their mean area under the ROC curve (AUC_{ROC}) and their matches to the LIPID MAPS structure database bulk search (mass, delta, name, and formula). If applicable the ion. retention time (RT), exact MS1 mass (measured mass), and delta to the matched reference mass are given for lipids that could be identified in the LC-MS/MS data by exact mass measurement and database hits for their respective MS2 fragmentation (gray highlights).

mice (129S6/SvEvTac). Since lack of CL in adipose tissue leads to attenuated expression of UCP1,[7] we asked whether vice versa lack of UCP1 expression would affect CL metabolism. Therefore, we housed UCP1-WT and UCP1-KO mice at 23 °C, or cold acclimatized mice to 5 °C (**Figure 3**A). Subsequently, we investigated the presence and distribution of both CL 68:3 and CL 68:4 applying our MALDI-MSI protocol. The UCP1-IHC staining revealed the expected increase in UCP1 expression upon cold stimulation in UCP1-WT mice while no UCP1 could be detected in UCP1-KO mice in neither condition (Figure 3B, additional mouse examples Figures S3 and S4, Supporting Information). Analysis of the MALDI images for CL 68:4 (*m/z* 1401,805 ± 0.338 Da) and CL 68:3 (*m/z* 1403,834 ± 0.338 Da) confirmed a strong spatial overlap with the expression pattern of UCP1 in wildtype animals (Figure 3C,D, additional mouse examples Figures S3 and S4, Supporting Information). The relative intensities of both CL species were increased in cold acclimatized mice as compared to controls kept at 23 °C (Figures 3C,D and 4, additional mouse examples Figures S3 and S4, Supporting Information). Interestingly, both CL species were also increased in cold acclimatized UCP1-KO animals. Their intensities tended to be even higher than in cold acclimatized UCP1-WT mice, as observed in all three biological replicates (**Figure 4**). The MALDI images revealed that even in UCP1 ablated mice the increased abundance of CLs was not ubiquitous but exhibited a spatial pattern similar to that of UCP1-WT mice.

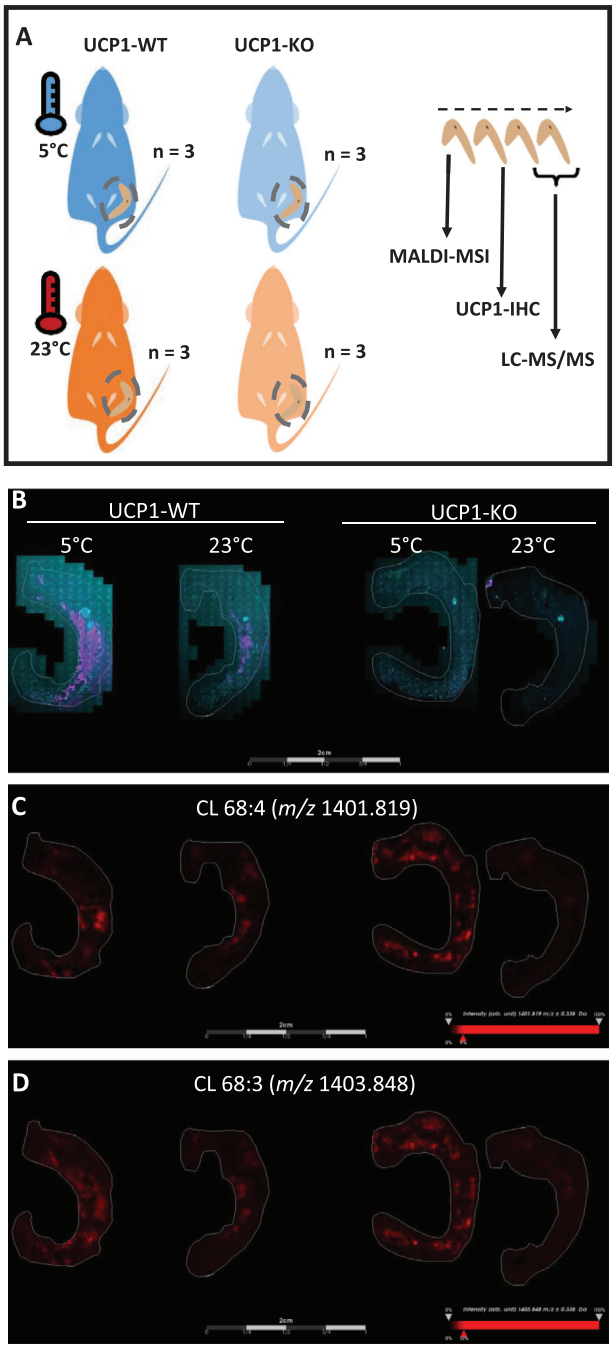

Figure 3. CL 68:4 and CL 68:3 abundance is associated with cold, independent of UCP1. A) Overview of the experimental setup. UCP1 knockout (UCP1-KO) and UCP1 wildtype (UCP1-WT) mice are either housed at 23 °C or acclimatized to 5 °C. iWAT is dissected (gray dashed circle). Four consecutive sections are prepared, the first used for MALDI-MSI, the second for IHC staining of UCP1, and the last two for LC-MS/MS analysis. B) IHC staining against UCP1 (magenta) and a Hoechst nuclear stain (cyan) of UCP1-WT and UCP1-KO mice. C–D) MALDI images of (C) m/z 1401.819 ± 0.338 Da representing CL 68:4 and D) m/z 1403.848 ± 0.338 Da representing CL 68:3.

Conclusively, we could demonstrate that the cardiolipins CL 68:3 and CL 68:4, as two distinct representatives of a well-established mitochondrial signature lipid class, are upregulated by cold exposure in iWAT of mice, independently of UCP1.

4. Discussion

The aim of this study was to characterize the lipid composition of WAT on a region-specific level in an in vivo context. Inguinal WAT is a highly heterogenous tissue,[14] a hallmark feature so far unaddressed by most lipidomic studies using whole tissue homogenates[7,8] or in vitro differentiated pre-adipocytes.[6,11] We made use of the MALDI-MSI technology, enabling the local acquisition of mass spectra on tissue sections to address this shortcoming. The feasibility of MALDI-MSI to investigate adipose tissue metabolism has recently been demonstrated on WAT of rats.[23] We demonstrate that the lipid composition of iWAT is regionally different, strongly resembling the heterogeneous spatial distribution of white and brite adipocytes and UCP1 expression in the tissue.[14] Combining MALDI-MSI with IHC and high-resolution LC-MS/MS, we could demonstrate that the lipid species CL 68:3 and CL 68:4 strongly co-localize with the expression of UCP1 in cold acclimatized 129S6/SvEvTac mice. Further investigation of UCP1-WT and UCP1-KO mice however demonstrated cold-induced upregulation of CL in iWAT independent of UCP1.

We detected several m/z intervals with overall highly similar regional distribution in different measurement runs and biological replicates, demonstrating the reliability of our MALDI-MSI approach. In line with the fat storage function of adipose tissue, the main verified lipid species were DG and TG. As such, we identified TG 44:1 (m/z 749.422) as a lipid species not specific to UCP1-positive or UCP1-negative regions but rather ubiquitously distributed. In contrast, m/z 774.388 showed a highly regional localization and was associated with the lymph node. This mass could be mapped to two potential glycerophospholipids (PC 36:8, PS 35:2) based on our LC-MS/MS data. Further, we demonstrate that TG is associated with UCP1-negative regions while DG is associated with regions with detectable UCP1 expression. This co-localization pattern may reflect regional differences in metabolic activity and function as UCP1 dependent thermogenesis is activated and fueled by free fatty acids derived from lipolysis.[2] Thus, regions rich in TG are potentially characterized by white adipocytes and DG-rich regions by UCP1 expressing brite adipocytes. In line with our findings, two DG associated with UCP1 in this study (DG 32:0 & DG 32:1) were also more abundant in vitro differentiated brite compared to white adipocytes.[6]

The upregulation of CL in cold acclimatized mice and its association to thermogenesis is well established.[6–9] Further, CL are bound to UCP1 and are important for its stability in the inner mitochondrial membrane, facilitating its function.[12,13] Thus, it is plausible that we detected CL 68:3 and CL 68:4 in close spatial association with UCP1 expression in iWAT of cold acclimatized mice. Intriguingly, application of our combined MALDI-MSI/UCP1-IHC/LC-MS/MS approach on UCP1-KO and UCP1-WT mice demonstrated for the first time that the cold-induced upregulation of CL is independent of UCP1. We speculate that CL 68:3 and CL 68:4 are generally associated with the

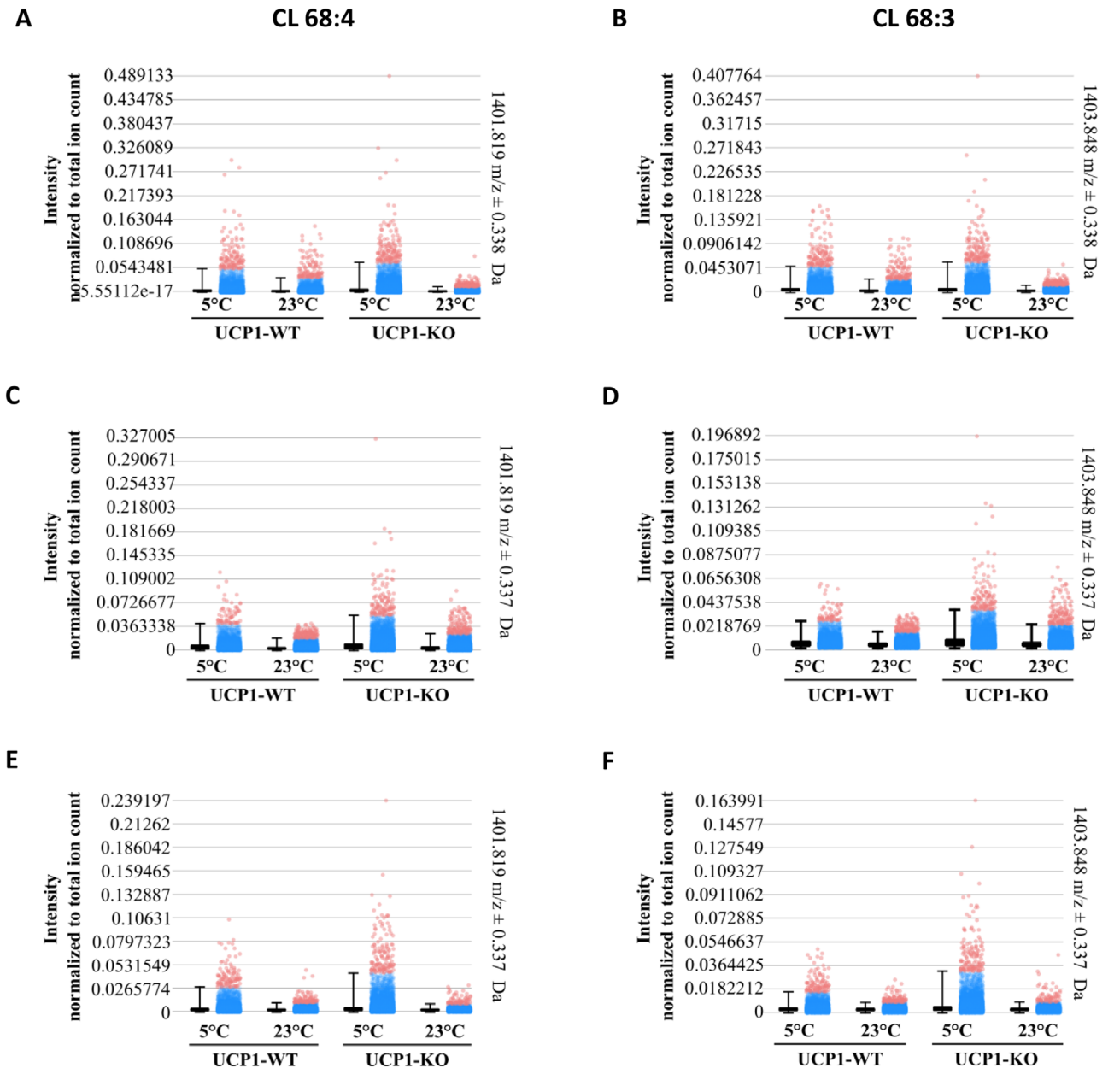

Figure 4. CL 68:3 and CL 68:4 are increased in cold acclimatized UCP1-KO mice. Intensities of (A,C,E) *m/z* 1401.819 and (B,D,F) *m/z* 1403.848 corresponding to the respective MALDI images. A) Figure 3, B) Figure 3D, C) Figure S3C, Supporting Information, D) Figure S3D, Supporting Information, E) Figure S4C, Supporting Information, and F) Figure S4D, Supporting Information.

cold-induced emergence of multilocular brite adipocytes rather than the expression of UCP1. In fact, multiple studies have meanwhile demonstrated that these cells have increased mitochondrial content, provide UCP1-dependent and -independent NST and occur in greater number in UCP1-KO compared to UCP1-WT mice.[24,25] Fully in line with these observations, CL 68:3 and CL 68:4 clearly tended to be more abundant in iWAT of cold-exposed UCP1-KO compared to WT mice. This strongly suggests that these two lipid species as members of a mitochondrial signature lipid class are novel surrogate markers for the recruitment of brite adipocytes and NST.

Despite these compelling results, there are some limitations to our study pertaining to the physiological implications. We exclusively studied iWAT and therefore are not able to elaborate if the observed spatial upregulation of CL is a regional phenomenon specific for iWAT, or also applies to other WAT depots prone to browning, or even other tissues capable to perform NST such as skeletal muscle. Furthermore, upregulation of CL in the absence of UCP1 may indicate a crucial function for alternative UCP1-independent mechanisms of thermogenesis such as futile fatty acid-triacylglyceride cycling by simultaneous lipolysis and reesterification,[26] Ca^{2+}[27] cycling, or

creatine-phosphate cycling[5] which all require sufficient mitochondrial capacity for oxidative phosphorylation. It will be of interest to follow up whether CL 68:3 and CL 68:4 are also associated with molecular markers of these alternative UCP1-independent mechanisms, or can be detected in other high metabolic rate tissues or in plasma. On the technological side, a further major limitation of our study is the low resolution of our MALDI-MSI device. In most instances, this resulted in the annotation of multiple possible lipid species for a single m/z interval. While we are confident about the annotation of the DG and TG based on their high abundance, this is a major limitation for low abundant or regionally very restricted lipids. These might be below the detection limit for the LC-MS/MS due to the dilution in the whole section homogenate. Other reasons for a lack of annotation or detection by LC-MS/MS include that m/z intervals provided by the MALDI-MSI do not necessarily reflect lipid species but peptide fragments. Additionally, a lack of annotated database references might further explain why for some m/z intervals no annotated lipid species could be identified in our LC-MS/MS data set. These issues are already resolved by the advancement of MALD-MSI instrumentation with higher resolution, MS2 spectra, and ion mobility.

5. Conclusion

Applying our MALDI-MSI approach, we demonstrate that the previously reported cold-induced upregulation of CL in WAT[7,8] is a spatial phenomenon occurring independently of UCP1 expression. Conclusively, we demonstrate that MALDI-MSI is a powerful tool to investigate the relationship of lipid metabolism and functional characteristics of adipose tissue in an in vivo context.

Supporting Information

Supporting Information is available from the Wiley Online Library or from the author.

Acknowledgements

The authors highly appreciate the excellent work of Brigitte Weidenthaler and Alena Freudenmann testing and validating the immunohistochemistry and the MALDI-MSI workflows. This work was supported by a joint grant "Nutribrite" Deutsche Forschungsgemeinschaft ID: KL973/13-1 and French Agence Nationale de la Recherche ANR-15-CE14-0033, and by the Else Kröner-Fresenius Stiftung 2017_A108 - EKFZ.

Open access funding enabled and organized by Projekt DEAL.

Conflict of Interest

The authors declare no conflict of interest.

Ethics

All animal experimentation was performed according to the German animal welfare law with permission from the district government of Upper Bavaria (Regierung von Oberbayern, reference number ROB-55.2-2532.Vet_02-16-166).

Author Contributions

S.D. designed the study, performed mouse experiments, sectioning, immunohistochemistry, data analysis, interpreted the results and drafted the manuscript. K.K. performed MALDI-MSI and LC-MS/MS measurements, contributed to data analysis and revised the manuscript. S.M. conceived the study and performed mouse experiments. M.K. acquired funding, contributed to data interpretation and revised the manuscript. All authors approved the final version of the manuscript.

Data Availability Statement

The LC-MS/MS datasets for this study can be found in the MassIVE repository http://massive.ucsd.edu/ProteoSAFe/status.jsp?task=80d0ff4f33714268b486f540c41d4841). Other data supporting the findings of this study are available from the corresponding author upon reasonable request.

Keywords

brite adipocytes, cardiolipin, MALDI-MSI, uncoupling protein 1, white adipose tissue

Received: April 16, 2021
Revised: August 26, 2021
Published online: September 21, 2021

[1] M. Klingenspor, *Exp. Physiol.* **2003**, *88*, 141.
[2] B. Cannon, J. Nedergaard, *Physiol. Rev.* **2004**, *84*, 277.
[3] N. Petrovic, T. B. Walden, I. G. Shabalina, J. A. Timmons, B. Cannon, J. Nedergaard, *J. Biol. Chem.* **2010**, *285*, 7153.
[4] S. M. Jung, J. Sanchez-Gurmaches, D. A. Guertin, in *Brown Adipose Tissue* (Eds: A. Pfeifer, M. Klingenspor, S. Herzig), Handbook of Experimental Pharmacology *251*, Springer International Publishing, Cham **2019**, p. Brown Adipose Tissue Development and Metabolism 3, https://doi.org/10.1007/164_2018_168.
[5] L. Kazak, E. T. Chouchani, M. P. Jedrychowski, B. K. Erickson, K. Shinoda, P. Cohen, R. Vetrivelan, G. Z. Lu, D. Laznik-Bogoslavski, S. C. Hasenfuss, S. Kajimura, S. P. Gygi, B. M. Spiegelman, *Cell* **2015**, *163*, 643.
[6] S. Schweizer, G. Liebisch, J. Oeckl, M. Hoering, C. Seeliger, C. Schiebel, M. Klingenspor, J. Ecker, *PLoS Biol.* **2019**, *17*, e3000412.
[7] E. G. Sustarsic, T. Ma, M. D. Lynes, M. Larsen, I. Karavaeva, J. F. Havelund, C. H. Nielsen, M. P. Jedrychowski, M. Moreno-Torres, M. Lundh, K. Plucinska, N. Z. Jespersen, T. J. Grevengoed, B. Kramar, J. Peics, J. B. Hansen, F. Shamsi, I. Forss, D. Neess, S. Keipert, J. Wang, K. Stohlmann, I. Brandslund, C. Christensen, M. E. Jørgensen, A. Linneberg, O. Pedersen, M. A. Kiebish, K. Qvortrup, X. Han, et al., *Cell Metab.* **2018**, *28*, 159.
[8] M. D. Lynes, F. Shamsi, E. G. Sustarsic, L. O. Leiria, C. H. Wang, S. C. Su, T. L. Huang, F. Gao, N. R. Narain, E. Y. Chen, A. M. Cypess, T. J. Schulz, Z. Gerhart-Hines, M. A. Kiebish, Y. H. Tseng, *Cell Rep.* **2018**, *24*, 781.
[9] P. He, B. Hou, Y. Li, C. Xu, P. Ma, S. M. Lam, V. Gil, X. Yang, X. Yang, L. Zhang, G. Shui, J. Song, G. Qiang, C. W. Liew, G. Du, *Biomolecules* **2019**, *9*, 444.
[10] G. Paradies, V. Paradies, F. M. Ruggiero, G. Petrosillo, *Cells* **2019**, *8*, 728.
[11] L. Liaw, I. Prudovsky, R. A. Koza, R. V. Anunciado-Koza, M. E. Siviski, V. Lindner, R. E. Friesel, C. J. Rosen, P. R. S. Baker, B. Simons, C. P. H. Vary, *J. Cell. Biochem.* **2016**, *2193*, 2182.

[12] T. Hoang, M. D. Smith, M. Jelokhani-Niaraki, *J. Biol. Chem.* **2013**, *288*, 36244.
[13] Y. Lee, C. Willers, E. R. S. Kunji, P. G. Crichton, *Proc. Natl. Acad. Sci. USA* **2015**, *112*, 6973.
[14] C. Barreau, E. Labit, C. Guissard, J. Rouquette, M. L. Boizeau, S. Gani Koumassi, A. Carrière, Y. Jeanson, S. Berger-Müller, C. Dromard, F. Plouraboué, L. Casteilla, A. Lorsignol, *Obesity* **2016**, *24*, 1081.
[15] W. C. Skarnes, B. Rosen, A. P. West, M. Koutsourakis, W. Bushell, V. Iyer, A. O. Mujica, M. Thomas, J. Harrow, T. Cox, D. Jackson, J. Severin, P. Biggs, J. Fu, M. Nefedov, P. J. De Jong, A. F. Stewart, A. Bradley, *Nature* **2011**, *474*, 337.
[16] S. J. Pettitt, Q. Liang, X. Y. Rairdan, J. L. Moran, H. M. Prosser, D. R. Beier, K. C. Lloyd, A. Bradley, W. C. Skarnes, *Nat. Methods* **2009**, *6*, 493.
[17] S. Dieckmann, A. Strohmeyer, M. Willershaeuser, S. Maurer, W. Wurst, S. Marschall, M. Hrabe de Angelis, R. Kuehn, A. Worthmann, M. M. Fuh, J. Heeren, N. Koehler, J. Pauling, M. Klingenspor, *bioRxiv* **2021**, bioRxiv 2021.06.30.450595; https://doi.org/10.1101/2021.06.30.450595.
[18] M. Witting, T. V. Maier, S. Garvis, P. Schmitt-Kopplin, *J. Chromatogr. A* **2014**, *1359*, 91.
[19] H. Tsugawa, K. Ikeda, M. Takahashi, A. Satoh, Y. Mori, H. Uchino, N. Okahashi, Y. Yamada, I. Tada, P. Bonini, Y. Higashi, Y. Okazaki, Z. Zhou, Z. J. Zhu, J. Koelmel, T. Cajka, O. Fiehn, K. Saito, M. Arita, M. Arita, *Nat. Biotechnol.* **2020**, *38*, 1159.
[20] T. Alexandrov, M. Becker, S.-O. Deininger, G. Ernst, L. Wehder, M. Grasmair, F. von Eggeling, H. Thiele, P. Maass, *J. Proteome Res.* **2010**, *9*, 6535.
[21] M. Hoene, J. Li, H. U. Häring, C. Weigert, G. Xu, R. Lehmann, *Biochim. Biophys. Acta, Mol. Cell Biol. Lipids* **2014**, *1841*, 1563.
[22] M. D. Lynes, L. O. Leiria, M. Lundh, A. Bartelt, F. Shamsi, T. L. Huang, H. Takahashi, M. F. Hirshman, C. Schlein, A. Lee, L. A. Baer, F. J. May, F. Gao, N. R. Narain, E. Y. Chen, M. A. Kiebish, A. M. Cypess, M. Blüher, L. J. Goodyear, G. S. Hotamisligil, K. I. Stanford, Y. H. Tseng, *Nat. Med.* **2017**, *23*, 631.
[23] A. Fernández-Vega, E. Chicano-Gálvez, B. M. Prentice, D. Anderson, F. Priego-Capote, M. A. López-Bascón, M. Calderón-Santiago, M. S. Avendaño, R. Guzmán-Ruiz, M. Tena-Sempere, J. A. Fernández, R. M. Caprioli, M. M. Malagón, *Talanta* **2020**, *219*, 121184.
[24] R. Anunciado-Koza, J. Ukropec, R. A. Koza, L. P. Kozak, *J. Biol. Chem.* **2008**, *283*, 27688.
[25] J. G. Granneman, M. Burnazi, Z. Zhu, L. A. Schwamb, *Am. J. Physiol.: Endocrinol. Metab.* **2003**, *285*, E1230.
[26] S. Schweizer, J. Oeckl, M. Klingenspor, T. Fromme, *Life Sci. Alliance* **2018**, *1*, e201800136.
[27] J. Ukropec, R. P. Anunciado, Y. Ravussin, M. W. Hulver, L. P. Kozak, *J. Biol. Chem.* **2006**, *281*, 31894.